Decentralized Stablecoins and Collateral Risk *

Roman Kozhan† and Ganesh Viswanath-Natraj‡

First version: June 17, 2021 (posted SSRN)

This version: April 8, 2025 (posted SSRN)

Abstract

We analyze the mechanisms governing the price stability of MakerDAO's DAI, the first decentralized stablecoin. DAI is issued through overcollateralized debt positions (CDPs), where users borrow against cryptocurrency collateral. We show how peg-price deviations arise in equilibrium due to speculators' price pressure and limits to arbitrage. Using CDP-level data, we distinguish speculators from arbitrageurs and demonstrate how these constraints impact price stability. Introducing stable collateral and a direct conversion mechanism between DAI and stable collateral alleviates arbitrage frictions, improving peg stability while highlighting the inherent trade-off between decentralization and arbitrage design.

Keywords: Cryptocurrency, fixed exchange rates, monetary policy, stablecoins, collateralized debt positions.

JEL Classifications: F31, G14, G15, G18, G23

*For help with obtaining data for this project, we would like to thank Mike McDonald, Lou Kerner, and members from the MakerDAO team, Greg Di Prisco and Kenton Prescott. The views expressed in this paper are independent to MakerDAO. For detailed comments, we thank discussants Yeguang Chi, Oliver Gloede, Simon Mayer, Gustavo Schwenkler, Faten Ben Slimane, Zhuo Zhong, and Adrien d'Avernas, Dirk Baur, Bruno Biais, Agostino Capponi, Jonathan Chiu, Darrell Duffie, Barry Eichengreen, Hermann Elendner, Jean Flemming, Pierre-Olivier Gourinchas, Jorge Herrada, Engin Iyidogan, Brett Lyons, Rich Lyons, Andreas Park, Ingolf Pernice, Bryan Routledge, Fahad Saleh, David Skeie, Ruslan Sverchkov, Quentin Vandeweyer, Junxuan Wang, and seminar participants at the Australasian Banking and Finance Conference, Australian National University, Bayes Business School, CBER Blockchain conference, CEBRA annual meeting, the 17th Central Bank Conference on the Microstructure of Financial Markets, Federal Reserve Board, French Finance Association, New Zealand Finance Conference, NYU Tokenomics Conference, Office of Financial Research, San Francisco Fintech Conference, UCL Blockchain Conference, University of Southampton Cryptocurrency Conference, the University of Western Australia Blockchain Conference and Weizenbaum Institut. We thank Amit Chaudhary for valuable research assistance.

†Warwick Business School, The University of Warwick, Scarman Road, Coventry CV4 7AL, UK. E-mail: Roman.Kozhan@wbs.ac.uk

‡Warwick Business School, The University of Warwick, Scarman Road, Coventry CV4 7AL, UK. E-mail: ganesh.viswanath-natraj@wbs.ac.uk

1 Introduction

Stablecoins are a class of cryptocurrencies designed to maintain a stable peg to a financial asset, typically the US dollar. While most stablecoins rely on a centralized issuer, decentralized stablecoins – led by MakerDAO's DAI – have grown significantly in recent years, with a market capitalization exceeding 5 billion USD.[1]

Unlike centralized stablecoins, DAI issuance is decentralized and governed by autonomous smart contracts on the Ethereum blockchain.[2] DAI tokens are generated when an investor deposits collateral, typically Ether (ETH), into a collateralized debt position (CDP). Based on the value of collateral, an investor can issue (borrow) a certain amount of DAI tokens.

Decentralized stablecoins offer a potential alternative to centralized stablecoins (such as Tether or USDC) by eliminating custodial risk – the risk that a centralized issuer mismanages or absconds with funds – and mitigating the associated run risks and redemption inefficiencies (see Ma, Zeng, and Zhang, 2023; Gorton, Ross, and Ross, 2022 for a discussion). However, decentralized stablecoins also have inherent limitations due to the design of arbitrage mechanisms necessary for peg stability. In particular, an arbitrageur who wishes to exploit an arbitrage opportunity by issuing DAI and selling it in the market has to post collateral, which exposes her to potential collateral losses.

We outline two key contributions in analyzing the fundamental trade-off between decentralization and arbitrage design in stablecoins. First, while DAI's decentralized issuance mechanism eliminates custodial risk, it remains exposed to collateral risk arising from fluctuations in the value of underlying assets. On one hand, speculators who use DAI to leverage or short collateral assets exert price pressure in secondary markets, destabilizing the peg. On the other hand, arbitrageurs cannot entirely eliminate these peg deviations due to limits to arbitrage stemming from the scarcity of arbitrage capital (see Gromb and Vayanos, 2002) and exposure to expected collateral losses and liquidation risk. These frictions are particularly pronounced when arbitrageurs are constrained to use

1. Market capitalization of $5.4 billion USD as of September 16, 2024, based on the author's calculations. This date also marks the end of our sample period, which coincides with the rebranding of DAI and the migration of its supply to a new stablecoin. Since September 2024, DAI has been rebranded as *Sky*. See MakerDAO Sky Rebranding Overview.

2. A smart contract is a set of self-executing instructions, written in code, that define contract conditions for each counterparty under various scenarios. Since it is publicly visible on the blockchain, it can be verified by all network participants.

only risky collateral.

Second, we demonstrate that limits to arbitrage are salient: arbitrageurs cannot entirely eliminate deviations from par even after the introduction of stable collateral types (such as the centralized stablecoin USDC) in March 2020. While stable collateral reduces expected losses and liquidation risk, arbitrage remains constrained in the absence of an immediate and costless mechanism to convert mispriced DAI into a replicating asset or portfolio. In such cases, arbitrageurs must invest scarce capital, lock it up for a period, and rely on eventual price convergence—exposing them to opportunity costs and residual risk.

The introduction of the Peg Stability Module (PSM) in December 2020 directly addresses this friction by enabling 1:1 swaps between DAI and USDC. This facility removes the timing uncertainty and execution risk of arbitrage trades, effectively closing the gap between DAI and its target price. However, this improvement comes at the cost of re-centralization: DAI becomes increasingly dependent on USDC's operational stability and reserve backing. Our findings suggest that some degree of re-centralization is necessary to support effective arbitrage and sustain peg stability, underscoring the structural limitations of fully decentralized stablecoins or private money systems.

To motivate our analysis, we present stylized facts on the DAI stablecoin peg in Figure 1, partitioning the sample into pre- and post–PSM periods. Prior to the PSM, the distribution of DAI peg deviations exhibited a pronounced positive skew, with the peg trading at an average premium of approximately 100 basis points. Unlike other stablecoins—which often trade at a discount due to redemption risk and concerns over the solvency of custodial reserves—DAI frequently traded above par. This premium persisted even after the introduction of stable collateral types, such as USDC, in March 2020. By contrast, in the post-PSM period beginning in December 2020, the distribution of peg deviations becomes more symmetric and tightly centered around the \$1.00 par value. The introduction of a direct arbitrage channel via the PSM has improved peg stability.

To rationalize these facts on the DAI peg, we develop a simple model based on the interaction between two types of agents: risky cryptocurrency speculators and arbitrageurs. Speculators use DAI to implement leveraged long or short positions in ETH (or other volatile cryptocurrencies). When expected ETH returns are high, speculators enter leveraged long positions by depositing ETH as collateral in a protocol, borrowing DAI, and

selling it in the secondary market. This increases DAI supply and places downward pressure on the peg. When expected ETH returns are low, speculators short ETH by purchasing DAI in the secondary market, depositing it in a lending protocol (e.g., Compound or Aave), borrowing ETH, and selling it. This demand for DAI places upward pressure on the peg. As a result, speculative demand for DAI is positively correlated with expected ETH returns.

Arbitrageurs, by contrast, attempt to exploit deviations from the peg. However, they face constraints due to scarce capital and the absence of a direct redemption mechanism between DAI and the U.S. dollar. These frictions limit arbitrage capacity and allow peg deviations to persist.

We hypothesize that both DAI borrowing and the DAI price respond to speculators' expectations of future ETH returns. The introduction of stable collateral types weakens this link by allowing arbitrageurs to take more stable, low-risk positions against peg deviations, thereby improving peg efficiency. Finally, the introduction of a direct conversion mechanism—such as the PSM—anchors DAI to the stable collateral. However, this shifts the peg stability from market-based arbitrage to the credibility and stability of the collateral itself.

We present empirical evidence supporting the role of the speculative channel in DAI price stability. Using the complete transaction history of individual CDPs, we disentangle speculators from arbitrageurs by analyzing borrowing behavior across collateral types. Speculators predominantly use ETH (or other volatile assets) as collateral, borrowing DAI to take leveraged positions in risky assets. We show that their borrowing is positively associated with expected ETH returns, confirming their role in driving speculative cycles. In contrast, arbitrageurs primarily rely on stable collateral, such as USDC, borrowing DAI to exploit price premia rather than to speculate on ETH price movements. We find that arbitrage-driven borrowing is negatively associated with expected ETH returns, reinforcing the distinction between speculative and arbitrage-based borrowing strategies.

Next, we assess the limits to arbitrage and their impact on peg efficiency. We document a significant negative correlation between DAI prices and expected ETH returns, confirming that speculative activity drives deviations from the peg. These effects persist even after controlling for alternative demand-side factors from secondary markets and protocol-driven liquidations (triggered when undercollateralized CDPs are forcibly closed

and collateral is sold to repurchase DAI). While both of these mechanisms can lead to peg deviations, our results indicate that speculative dynamics remain the dominant force.

To formally account for simultaneity and feedback effects among key drivers of the DAI price, we estimate a Structural Vector Autoregression (SVAR) model. The SVAR confirms that expected ETH return shocks are the most robust and persistent source of peg deviations under risky collateral regimes, while liquidation volumes and demand-side proxies exhibit weaker or short-lived effects. These results reinforce our interpretation that limits to arbitrage constrain the ability of market participants to offset speculative price pressure in real-time.

Finally, we evaluate how collateral risk affects arbitrage efficiency by examining the role of stable collateral in improving peg stability. We show that the introduction of stable collateral types weakens the link between the DAI peg and expected ETH returns, thereby improving peg efficiency. Specifically, a 1% increase in the share of stable collateral reduces the absolute value of DAI price deviations by approximately 0.3 basis points. Most of this improvement is driven by the increasing share of PSM-based collateral. Moreover, the introduction of the PSM effectively eliminates the correlation between the DAI price and expected ETH returns. However, this improvement comes at the cost of increased vulnerability to USDC-specific risks: during episodes of USDC de-pegging, DAI tends to trade at a discount.

Overall, our findings highlight a fundamental trade-off between decentralization and peg efficiency. While crypto-collateral preserves decentralization, it limits arbitrage and exposes the peg to speculative pressures. Introducing stable collateral and direct conversion mechanisms improves peg stability but at the cost of increased reliance on centralized assets.

Related Literature. The empirical research most relevant to our paper investigates the properties of stablecoins, its susceptibility to devaluation risk and comparisons to traditional money markets (Dell'Erba, 2019; Arner, Auer, and Frost, 2020; Frost, Shin, and Wierts, 2020; Force et al., 2020; Hoang and Baur, 2020; Barthelemy, Gardin, and Nguyen, 2021; Gorton, Ross, and Ross, 2022; Gorton et al., 2022; Eichengreen, Nguyen, and Viswanath-Natraj, 2023; Oefele, Baur, and Smales, 2024), arbitrage in stablecoin and cryptocurrency markets (Lyons and Viswanath-Natraj, 2023; Makarov and Schoar, 2019, 2020; Borri and Shakhnov, 2018; Pernice and Anton, 2021; Ma, Zeng, and Zhang,

2023), governance and voting behavior in decentralized stablecoin protocols (Gu, Raghuvanshi, and Boneh, 2020; Zhao et al., 2022; Sun, Stasinakis, and Sermpinis, 2024), and theoretical work that modeles the price dynamics of stablecoins (Routledge and Zetlin-Jones, 2021; Klages-Mundt and Minca, 2020; Li and Mayer, 2020; d'Avernas, Bourany, and Vandeweyer, 2022; Bertsch, 2023).

We relate to empirical work on understanding and quantifying the run-risk of stablecoins (Gorton et al., 2022; Eichengreen, Nguyen, and Viswanath-Natraj, 2023; Ma, Zeng, and Zhang, 2023). While these frameworks are useful at understanding the sources of redemption behavior on stablecoin pegs, they cannot reconcile the fact that the DAI peg, prior to the introduction of stable collateral types, experienced significant premiums. Our paper rationalizes DAI premiums through a model framework whereby speculators who borrow DAI to take leveraged positions can lead to systematic fluctuations of the DAI peg. We argue that stablecoins backed by volatile collateral lack a reliable arbitrage mechanism, making collateral risk a key limit to arbitrage. We show that the inclusion of stable collateral types strengthens arbitrage efficiency and improves peg stability.

Turning to theoretical models, Routledge and Zetlin-Jones (2021) apply a speculative attack framework to stablecoins, and find that centralized stablecoin regimes can collapse if investors expect insufficient dollar reserves. Li and Mayer (2020) examine a centralized issuer of dollar-backed stablecoins that autonomously controls token supply and maximizes dividends for governance token holders. They find that open market operations, reserve management, and over-collateralization can help prevent speculative attacks and peg discounts. d'Avernas, Bourany, and Vandeweyer (2022) analyze equilibrium conditions in which both fiat-backed and decentralized crypto-backed stablecoins maintain parity following demand shocks or collateral liquidations. In the context of decentralized stablecoins, they show that governance-managed buffer reserves function as a stabilizing mechanism to restore peg stability, similar to central bank reserve management.

Our paper contributes to this literature by demonstrating the inherent limits to arbitrage in decentralized stablecoin design, and how access to stable collateral types can introduce arbitrage mechanisms necessary for stablecoin price stability.

Second, we contribute to the existing literature on DeFi (see (Harvey, Ramachandran, and Santoro, 2021; Schär, 2021; John, Kogan, and Saleh, 2023) for a survey). Research in this field has focused on decentralized stablecoins and DeFi lending protocols, such as

Compound and Aave, which use algorithmic mechanisms to set interest rates and allocate funds (Gudgeon et al., 2020; Perez et al., 2020; Qin et al., 2021; Lehar and Parlour, 2022; Chiu et al., 2022; Saengchote, 2023; Rivera, Saleh, and Vandeweyer, 2023; Chaudhary, Kozhan, and Viswanath-Natraj, 2023; Heimbach and Huang, 2024). DAI primarily functions as a savings instrument in lending protocols and as liquidity in decentralized exchange pools. Within this literature, we are the first to leverage comprehensive CDP transaction data to examine the determinants of individual CDP leverage and to distinguish between speculator and arbitrageur motives. Subsequent research on lending protocols supports the speculative channel proposed in our paper, showing that investors use DeFi lending platforms to take leveraged positions in a manner similar to leveraging with DAI.

While our primary focus in the DeFi literature is on understanding the speculative channel, another key outcome of our analysis is the necessity of some degree of re-centralization to improve arbitrage design. The theme of re-centralization has been explored in other contexts, such as mitigating front-running in decentralized exchanges (Capponi, 2024). A broader theme in DeFi is that while decentralization removes the need for intermediaries, it introduces inefficiencies that often require targeted forms of re-centralization to address. Our findings contribute to this discussion by demonstrating that stable collateral plays a crucial role in enhancing arbitrage efficiency and peg stability in decentralized stablecoins.

Finally, we contribute to a literature on arbitrage with financial constraints (Gromb and Vayanos, 2002, 2018; Brunnermeier and Pedersen, 2009; Nyborg and Rösler, 2019) and draw insights from Brunnermeier and Pedersen (2009) and Gromb and Vayanos (2018). Brunnermeier and Pedersen (2009) investigate the relationship between funding margins, asset prices, and market liquidity. Gromb and Vayanos (2018) show that shocks to arbitrage capital can increase spreads and risk-premia. Our paper's focus on the limit to arbitrage via the riskiness of collateral types adds to the existing literature on arbitrage with financial constraints. In particular, we exploit the introduction of the USDC collateral type in 2020, which led to a significant decline in peg-price deviations and volatility. In our paper, we contribute to this literature by showing empirically that risky collateral generates a limit to arbitrage.

The remainder of the paper is structured as follows. In Section 2 we provide institu-

tional details of MakerDAO protocol. In Section 3 we introduce a model framework to construct our research hypotheses. In Section 4 describe the data sources for our empirical work. In Section 5 we conduct our empirical analysis. Section 6 concludes.

2 Institutional Details and Definitions

2.1 DAI Creation and Liquidations

DAI Creation. To create DAI in the primary market, an investor can initiate a CDP by depositing a specific amount of collateral, such as ETH, into a vault. They are then able to borrow a fraction of their collateral as DAI tokens. The CDP's valuation of collateral and DAI borrowings is regulated by a set of autonomous contracts that adjust in real-time.

There are three primary use cases for DAI tokens. Firstly, DAI can be deposited as savings in the DAI savings protocol, where the MakerDAO protocol sets the DAI savings rate as a potential stability tool.[3] Secondly, DAI is a popular currency for use in decentralized finance (DeFi) protocols such as Compound, which employ algorithms to automatically set interest rates and allocate funds. As of 10 May 2021, over 4 billion USD of DAI savings have been lent in the Compound protocol, with lending rates hovering around 3% per annum.[4] Thirdly, DAI can be used as a vehicle currency to purchase and potentially leverage other cryptocurrencies, such as Bitcoin (BTC) and ETH.

To close a CDP position, an investor must first redeem all DAI tokens by either selling the investment currency for DAI tokens in the secondary market or redeeming their DAI tokens in DeFi Exchanges and lending protocols. Once all borrowed DAI tokens have been redeemed, the smart contract is adjusted to unlock the collateral, resulting in the closure of the CDP.[5]

Leverage Ratio and Liquidations. The MakerDAO system requires investors to over-collateralize their borrowings. The leverage ratio is calculated as the ratio of generated DAI (pegged at 1 USD) to the collateral value in USD, as shown in Equation (1):

$$\text{Leverage ratio} = \frac{\text{Generated DAI}}{\text{Collateral price} \times \text{Collateral amount}} \times 100 \tag{1}$$

3. Adjustments of the DAI savings rate is set by the MakerDAO protocol as a potential stability tool, which we discuss in more detail in a following section.
4. See compound.finance/markets for more details.
5. We outline the steps in creating DAI in a schematic in Appendix A.

If the collateral price falls, investors must either inject more collateral or redeem DAI to maintain their collateral level. Each vault has a maximum leverage ratio. For ETH collateral, the maximum DAI that can be borrowed is two-thirds of the dollar value of the ETH collateral.[6]

The MakerDAO system enforces an auction mechanism through smart contracts that liquidate under-collateralized vaults. A group of agents, known as keepers, triggers liquidation when a vault breaches its minimum collateral threshold. The collateral is then auctioned to cover the outstanding DAI and a liquidation penalty. The auction process consists of two phases: first, bidders offer to buy the collateral by bidding DAI, and once the required DAI amount is reached, bidders compete by accepting less collateral for the DAI bid. When an auction is settled, the highest bidder receives the sold collateral, and an amount of DAI equal to the loan and liquidation fees is burned. Any remaining collateral is returned to the vault owner.

Vault owners are incentivized to maintain low leverage to avoid liquidation events. They can set up price alerts for their collateral or implement automated rules to recapitalize their positions when collateral prices fall below a critical threshold.

In addition to repaying the loan, liquidated investors are charged penalty fees of up to 15% of the borrowed DAI. These costs create strong incentives to maintain sufficient collateral buffers. Large swings in collateral asset prices have historically triggered liquidation waves, sharp contractions in DAI borrowing, and peg premiums.[7] An illustrative example of a liquidation is provided in Appendix A.

2.2 System Parameters

Stable Collateral Types. On November 18, 2019, the MakerDAO protocol underwent a significant shift with the introduction of multiple collateral types. In addition to volatile assets like ETH, users could now post alternative forms of collateral such as WBTC—a tokenized version of Bitcoin on the Ethereum blockchain. On March 12, 2020, the Maker-

6. Note that the threshold leverage can differ based on the collateral type. For example, the threshold level of leverage for positions using USDC collateral is one. The economic design of leverage thresholds are similar to the practice of haircuts on collateral provided in Repurchase agreements (Repos), where risky collateral are typically discounted at high haircuts.

7. On 12 March 2020, for instance, ETH prices fell by nearly 50%, causing over $10 million in liquidations and an 8 percentage point spike in the DAI peg. Blockchain congestion and soaring gas fees—exceeding 100 GWEI, up from 10 GWEI the day before—prevented many users from adding collateral or repaying debt, leading to the liquidation of over 1,200 Vaults. For more, see MakerDAO's post-mortem.

DAO community also approved the inclusion of the stablecoin USDC, allowing for higher leverage through its fixed collateralization ratio of one.

USDC is issued by Circle and backed by a reserve of liquid assets, including U.S. Treasuries and cash held at regulated financial institutions.[8] While USDC has generally maintained a tight peg, its stability was temporarily disrupted in March 2023 following the collapse of Silicon Valley Bank, which held a portion of its cash reserves. This episode highlighted the residual risks of using centralized stablecoins as collateral, particularly during periods of financial stress.

Peg Stability Module. To incentivize the use of stable collateral, the Maker protocol introduced the Peg Stability Module (PSM) in December 2020. The PSM allows users to swap DAI for USDC at a 1:1 rate, effectively anchoring the DAI/USD peg to USDC. This eliminates the need to create a vault and deposit collateral, reducing complexity and liquidation risk. A technical difference between the PSM and having stable collateral type is liquidation risk. For example, if investors deposit USDC collateral into a vault, there is risk of a collapse of the USDC peg which can trigger a sufficient decline in the value of collateral and a liquidation event. By introducing this direct conversion mechanism as well as removing liquidation risk for investors, the PSM further removes limits to arbitrage and stabilizes the peg. However, users must pay a one-time fee, which incentivizes arbitrageurs to close peg-price deviations using the module.

The PSM differs from vault-based stable collateral in its treatment of liquidation risk. Depositing USDC as collateral in a vault exposes users to potential USDC de-pegging, which can trigger liquidation if its value declines. In contrast, the PSM shifts liquidation risk to the Maker Protocol, as it guarantees a 1:1 exchange rate even when USDC trades at a significant discount, providing a more secure option for users.[9]

Interest Rates. The MakerDAO protocol employs various interest rates to help control the DAI peg and manage supply and demand fluctuations. One such tool is the *stability fee*, which functions similarly to an interest rate set by a central bank but is determined through a decentralized governance process. Stability fee changes are approved via continuous voting, where participants select rate adjustments. If a proposed change receives sufficient votes, the new stability fee takes effect. This mechanism regulates the DAI

8. As of November 2024, Circle reported over $39 billion in reserves. See circle.com/transparency.
9. Further details on the PSM can be found at MakerDAO: Peg Stability Module Overview.

peg by influencing borrowing costs and overall system leverage—higher stability fees discourage borrowing, reducing leverage, while lower fees encourage borrowing and increase liquidity.

Another key mechanism is the *Dai Savings Rate* (DSR), which allows DAI holders to earn passive yield on their holdings. Unlike traditional interest-bearing accounts, the DSR is a smart contract feature that continuously distributes MakerDAO's revenue to depositors on every Ethereum block. The yield is funded by MakerDAO's profits and serves as an incentive to hold DAI.

Real World Assets. Tokenizing Real World Assets (RWAs) bridges traditional finance and DeFi, allowing off-chain assets to be represented and transacted on-chain. MakerDAO has increasingly integrated RWAs into its collateral framework to enhance capital efficiency and peg stability. This process involves converting USDC reserves into interest-bearing assets such as U.S. Treasury securities through intermediaries like Andromeda, with these holdings represented on-chain.[10]

The adoption of RWAs serves several key functions within MakerDAO's ecosystem. First, it diversifies collateral composition, reducing reliance on volatile assets like ETH and and exposure to de-pegging risk of stablecoins like USDC. Second, it improves capital efficiency by converting idle USDC reserves into yield-generating assets, mitigating the opportunity costs associated with non-productive reserves held in the PSM. Third, the additional revenue from RWAs enables MakerDAO to raise the DSR, incentivizing DAI adoption.

MakerDAO Auctions and Governance. The Maker governance protocol maintains system stability by adjusting risk parameters such as collateral types, liquidation ratios, debt ceilings, and stability fees. Governance decisions are made through MKR token voting, where each MKR token represents one vote, and votes are cast by locking MKR.

In addition to governance, MKR also functions as a backstop against liquidation shortfalls. For example, during the March 12 2020 *Black Thursday* event, auction mechanisms failed, leading to investor losses and destabilizing the system. This failure pressured the DAI peg, as keepers—who purchase collateral in exchange for DAI during auctions—faced

10. See MakerDAO's December 2023 RWA Report, which details MakerDAO's Treasury bill investments and its strategy for optimizing yield while maintaining decentralized collateralization. MakerDAO's RWA holdings include short-term U.S. Treasury bills, providing a stable source of yield while minimizing exposure to crypto market volatility.

a shortage of DAI liquidity and could not participate effectively.

To address such risks, MakerDAO introduced safeguards for scenarios in which liquidation auctions fail to recover sufficient funds. In these cases, the protocol can auction new MKR tokens to remove excess DAI from circulation, effectively conducting an open market operation that dilutes MKR's value.[11]

3 Model

To structure our testable hypotheses, we introduce a model with an aim to characterize the effect of speculative demand and limits to arbitrage on DAI peg instability.

We start with an economy featuring two assets: a collateralized stablecoin D (e.g., DAI) and a risky speculative asset E (e.g., ETH), both traded at times $t = 0, 1$. In the following section, we extend the model by allowing the arbitrageur to post an alternative stable asset as collateral. At time 0, stablecoin D trades at price p_D (determined in equilibrium) and at time 1 it pays off 1 USD with probability 1.[12] We assume that the market for the stablecoin D is small relative to E and does not affect pricing of E and so the price p_E of asset E is exogenously given. The gross return on asset E is a random variable R_E taking values of $\mu_E + \sigma_E$ or $\mu_E - \sigma_E$ with probability 0.5 each.

The stablecoin D is in zero net supply and in order to trade it in the secondary market, it first has to be issued in the protocol (e.g., MakerDAO). To do so, a trader has to open a CDP by depositing collateral into a protocol vault and receive a fraction θ of its value in D with $\theta \leq \bar{\theta}$. If at time 1, the value of collateral drops so that the ratio of issued stablecoin to collateral value exceeds $\bar{\theta}$, the protocol activates the liquidation of collateral and the investor is subject to penalty L. We assume that the penalty is prohibitively large so that traders will always avoid liquidations. This means that the effective upper bound on the leverage ratio is $\theta \leq \bar{\theta}(\mu_E - \sigma_E)$. To ensure that the liquidation risk matters but at the same time is not too severe to prevent the issuance of stablecoins, we assume that $\sigma_E < \mu_E < 1 + \sigma_E$.

11. For further information on Maker governance and the relationship between MKR price dynamics and system surplus, see Kozhan and Viswanath-Natraj (2022), which shows that higher surplus leads to MKR burning and increases in valuation.

12. This assumption is based on two points. First, the governance mechanism of the protocol (not modeled here) is designed to keep the peg via setting policy interest rates and issuance of the governance tokens. Second, although traders might have different beliefs about the future liquidation value, our model aims to derive an equilibrium price under the most favorable beliefs for the stability of asset D.

For expositional simplicity, we assume that all interest rates are equal to zero, although we control for interest rates in our empirical analysis later. We also abstract from any other costs (such as gas and swap fees).

Agents. There are two representative agents: a speculator and an arbitrageur. The speculator takes long or short positions in asset E based on their beliefs about its expected return, volatility, and the price of the stablecoin. The arbitrageur, by contrast, focuses exclusively on mispricing of the stablecoin D, taking long or short positions in D to profit from deviations from its peg. We assume that the arbitrageur does not trade in asset E and is solely concerned with arbitrage opportunities in the stablecoin market.

At time $t = 0$, the speculator holds an initial endowment of W_0^s in cash (denominated in US dollars). Depending on his expectation μ^s about the return on asset E (which might or might not equal to μ_E and depends on whether the speculator holds rational expectations), the speculator either holds a long or short position in E. The speculator leverages his long position if the expected value μ_E is high enough. To leverage his position by factor ω^s, he deposits asset E as collateral, borrows $\omega^s W_0^s$ stablecoins, sells them for $\omega^s p_D W_0^s$ US dollars and exchanges the US dollars for more units of asset E. When the position is liquidated at time 1, the speculator pays $\omega^s W_0^s$ to buy DAI (at price 1), releases collateral and converts it to the US dollars. His wealth W_1^s in this case evolves according to

$$W_1^s = W_0^s \left(R_E(1 + \omega^s p_D) - \omega^s \right), \quad 0 \leq \omega^s \leq \bar{\theta}. \tag{2}$$

If the leverage ratio is $\omega^s = 0$ then there is no supply of stablecoins and we set the price $p_D = 1$ (this happens when the speculator still holds a long position in asset E but does not find it optimal to leverage it). The first term in Equation (2) is the return earned on the leveraged position of asset E and the second term is the US dollar amount of stablecoin D that the speculator buys back to release his collateral at time 1.

When the speculator expects negative future returns, he takes a short position in asset E. To short $|\omega^s|$ (with $\omega^s < 0$) fraction of his wealth, he purchases $\frac{|\omega^s| W_0^s}{p_D}$ units of asset D in the secondary market and deposits them as collateral in a lending protocol (such as Compound or Aave). He then borrows asset E worth $|\omega^s| W_0^s$ in US dollar terms and sells

it in the secondary market.[13] When closing the short position, the speculator buys back the required number of units of asset E, releases $\frac{|\omega^s|W_0^s}{p_D}$ units of asset D from the lending protocol and converts it to the US dollars at price 1. His wealth W_1^s in this case becomes

$$W_1^s = \omega^s W_0^s \left(R_E - \frac{1}{p_D} \right), \quad -1 \leq \omega^s \leq 0. \tag{3}$$

The first term in Equation (3) measures the return from depreciation of asset E and the second term measures loss/gain of the speculator due to mispricing in D.

The speculator decides which strategy to choose (long or short) and the optimal demand coefficient ω^s by maximizing the mean-variance utility of W_1^s:

$$U(W_1^s) = \mathbb{E}[W_1^s] - \frac{\gamma}{2} Var[W_1^s] \tag{4}$$

subject to the evolution of wealth in Equations (2) and (3) and the corresponding constraints on ω^s.

The arbitrageur's role is to absorb excess demand and supply of stablecoins. When the speculator leverages his long position in asset E ($\omega^s > 0$), the arbitrageur takes a long position in stablecoin D (buys $\Delta^a > 0$ value of D) based on mispricing of the peg (and liquidates it at price 1 USD on date 1). Her wealth evolves according to

$$W_1^a = \Delta^a (1 - p_D) + W_0^a, \quad 0 \leq \Delta^a \leq W_0^s. \tag{5}$$

When the speculator buys stablecoins to short asset E, the arbitrageur takes a short position in stablecoins ($\Delta^a < 0$) by putting $\frac{\Delta^a}{\theta^a}$ value of asset E as collateral into the protocol vault and borrowing $|\Delta^a|$ value of asset D to sell to the speculator. In this case, the arbitrageur's terminal wealth depends on the return of the collateral asset:

$$W_1^a = -\frac{\Delta^a}{\theta^a} R_E + \Delta^a (1 - p_D) + W_0^s + \frac{\Delta^a}{\theta^a}, \quad 0 < -\Delta^a \leq \theta^a W_0^s \text{ and } 0 < \theta^a \leq \bar{\theta}(\mu_E - \sigma_E), \tag{6}$$

The arbitrageur is risk-neutral and competitive. She is rational and correctly perceives the parameters μ_E and σ_E. The only friction affecting the arbitrageur's ability is the

13. We assume no liquidation risk in the lending protocol to focus purely on frictions in the stablecoin market.

scarcity of the arbitrage capital which we model by assuming[14]

$$W_0^a < \bar{\theta}(1-\sigma_E)W_0^s. \tag{7}$$

Definition. An *equilibrium* is a price p_D such that ω^s maximizes the speculator's expected utility of the terminal wealth, Δ^a ensures non-negative expected profit of the arbitrageur subject to the constraints:

$$\Delta^a(1-p_D) \geq 0 \quad \text{(non-speculation of the arbitrageur)}, \tag{8}$$

$$\Delta^a = \omega^s W_0^s \quad \text{(market clearing condition)}. \tag{9}$$

Let us define

$$\mu^{(1)} = \min\left\{1, \frac{\bar{\theta}(\mu_E-\sigma_E)}{\bar{\theta}(\mu_E-\sigma_E)-(\mu_E-1)}\right\} - \gamma\sigma_E^2\bar{\theta}W_0^a(\mu_E-\sigma_E), \tag{10}$$

$$\mu^{(2)} = \frac{\bar{\theta}(\mu_E-\sigma_E)}{\bar{\theta}(\mu_E-\sigma_E)-(\mu_E-1)}, \tag{11}$$

$$\mu^{(3)} = 1+\gamma\sigma_E^2 W_0^s, \tag{12}$$

$$\mu^{(4)} = 1+\gamma\sigma_E^2(W_0^s+W_0^a). \tag{13}$$

Proposition 1: The equilibrium price and issuance of asset D are as follows:

- If $\mu_E \geq 1$ (the arbitrageur is optimistic about collateral expected return)

$$\begin{cases} p_D = \frac{1}{\mu^s+\gamma\sigma_E^2\bar{\theta}W_0^a(\mu_E-\sigma_E)}, & \Delta^a = \bar{\theta}W_0^a(\mu_E-\sigma_E), & \text{if } \mu^s < \mu^{(1)}, \\ p_D = 1, & \Delta^a = \frac{(1-\mu^s)}{\gamma\sigma_E^2}, & \text{if } \mu^s \in [\mu^{(1)}, 1), \\ p_D = 1, & \Delta^a = 0, & \text{if } \mu^s \in [1, \mu^{(3)}], \\ p_D = 1, & \Delta^a = \frac{\mu^s-1}{\gamma\sigma_E^2} - W_0^s, & \text{if } \mu^s \in (\mu^{(3)}, \mu^{(4)}], \\ p_D = \frac{\mu^s-\gamma\sigma_E^2W_0^s-\sqrt{(\mu^s-\gamma\sigma_E^2W_0^s)^2-4\gamma\sigma_E^2W_0^a}}{2\gamma\sigma_E^2W_0^a}, & \Delta^a = W_0^a, & \text{if } \mu^s > \mu^{(4)}. \end{cases} \tag{14}$$

- If $\mu_E < 1$ (the arbitrageur is pessimistic about collateral expected return)

14. This assumption effectively captures the liquidation risk for the speculator. Relaxing this assumption is equivalent to increasing the capital of the arbitrageur. We control for liquidations in the empirical analysis.

$$\begin{cases} p_D = \frac{1}{\mu^s + \gamma\sigma_E^2 \bar{\theta} W_0^a (\mu_E - \sigma_E)}, & \Delta^a = \bar{\theta} W_0^a (\mu_E - \sigma_E), & \text{if } \mu^s < \mu^{(1)}, \\ p_D = 1 - \frac{\mu_E - 1}{\bar{\theta}(\mu_E - \sigma_E)}, & \Delta^a = \frac{(1 - \mu^s p_D)}{\gamma\sigma^2 p_D}, & \text{if } \mu^s \in [\mu^{(1)}, \mu^{(2)}), \\ p_D = 1, & \Delta^a = 0, & \text{if } \mu^s \in [\mu^{(2)}, \mu^{(3)}], \\ p_D = 1, & \Delta^a = \frac{\mu^s - 1}{\gamma\sigma_E^2} - W_0^s, & \text{if } \mu^s \in (\mu^{(3)}, \mu^{(4)}], \\ p_D = \frac{\mu^s - \gamma\sigma_E^2 W_0^s - \sqrt{(\mu^s - \gamma\sigma_E^2 W_0^s)^2 - 4\gamma\sigma_E^2 W_0^a}}{2\gamma\sigma_E^2 W_0^a}, & \Delta^a = W_0^a, & \text{if } \mu^s > \mu^{(4)}. \end{cases} \tag{15}$$

Proof: See Appendix B.

The model generates different predictions depending on the relationship between parameters μ_E and μ^s. Before discussing different specifications, we outline the following implications.

No-trade region. The model predicts that there is a no-trade region whenever $\mu^s \in [1, \mu^{(3)}]$ if $\mu_E \geq 1$ or $\mu^s \in [\mu^{(2)}, \mu^{(3)}]$ if $\mu_E < 1$. The no-trade region always appears for moderately positive μ^s. This corresponds to cases when the speculator holds a long position in asset E but does not leverage it with the stablecoin. The width of the no-trade region is increasing with σ_E, W_0^s and decreasing with μ_E.

Price discounts. The stablecoin price discounts appear when μ^s is large enough. This happens because for large values of μ^s the speculator aggressively leverages his position in asset E and increases the supply of the stablecoin in the market. As the arbitrageur's capital is limited, for $\mu^s > \mu^{(4)}$, the supply of stablecoins exceeds the arbitrageur's capital W_0^a if the stablecoin were to trade at $p_D = 1$. In order to clear the market, the arbitrageur reduces the price which, in turn, reduces the demands of the speculator for E and hence the supply of D. It is also easy to see that p_D monotonically decreases with μ^s in this region:

$$\frac{\partial p_D}{\partial \mu^s} = \frac{1}{2\gamma\sigma_E^2 W_0^s} \left(1 - \frac{\mu^s - \gamma\sigma_E^2 W_0^s}{\sqrt{(\mu^s - \gamma\sigma_E^2 W_0^s)^2 - 4\gamma\sigma_E^2 W_0^a}} \right) < 0 \tag{16}$$

for any $\mu^s > \mu^{(4)}$. Finally, price discounts do not depend on μ_E since the arbitrageur does not have to use any collateral to exploit the mispricing.

Price premia. The stablecoin price premia might appear when μ^s is low enough. In this case, the speculator takes a short position in asset E and buys stablecoin in order to use it as collateral. The size of the short position depends on the speculators belief μ^s – the lower μ^s, the higher cost the speculator can bear as a result stablecoin overpricing. At the same time, the extent of the premium depends on the arbitrageur's willingness to supply stablecoin. The arbitrageur has to convert her USD capital into a collateral token

and lock it in the vault. Hence, the willingness of the arbitrageur to supply stablecoins depends on her expectation about the future performance of the collateral μ_E: the higher μ_E is, the lower is expected collateral loss for the arbitrageur and hence the lower the premium charged by her.

Next, we consider several variants of the model depending on investors' beliefs about asset E expected returns: rational expectations and heterogeneous beliefs.

3.1 Rational Expectations.

Consider the case where the speculator's belief about asset E is unbiased, such that $\mu^s = \mu_E$. Since our model is a single-period framework (i.e., it does not incorporate beliefs about future return dynamics), the rational expectations assumption simplifies to this condition.

The key implication of this assumption is the absence of trading (and hence stablecoin premia) when $\mu^s = \mu_E < 1$. In particular, the condition $\mu^s < \mu^{(2)}$ is never satisfied. The threshold $\mu^{(2)}$ itself becomes a function of μ_E and is only satisfied when $\mu_E < -\frac{\bar{\theta}\sigma^2}{1-\bar{\theta}}$. Intuitively, a decline in μ_E increases the expected collateral loss for the arbitrageur. It also reduces the amount of stablecoin the arbitrageur is willing to issue, due to a higher risk of liquidation—the upper bound on the leverage ratio, given by $\bar{\theta}(\mu_E - \sigma_E)$, decreases as μ_E falls. These two effects together raise the premium that the arbitrageur must charge to the speculator. This premium outweighs the potential profit from the speculator's short position. As a result, it becomes unprofitable to short-sell, and no trade occurs.

This result contrasts with empirical evidence, which shows that the price of DAI backed by a single risky collateral often exhibits substantial premia (see Figure 1). This observation rejects the assumption of rational expectations. An alternative explanation for the presence of DAI premia under rational expectations could be the existence of noise trading (not modeled here). However, in that case, the premia should not be systematically related to the expected return on asset E. We test this prediction in the following sections.

3.2 Heterogeneous Beliefs.

Consider the case where the speculator's beliefs about the expected return on asset E are influenced by sentiment, so that $\mu^s \neq \mu_E$. According to Proposition 1, the equilibrium outcome depends on whether $\mu_E \geq 1$ or $\mu_E < 1$.

Let $\mu^a \geq 1$. Unlike in the rational expectations benchmark, trade occurs in the heterogeneous beliefs model even when $\mu^s < 1$. This is because the arbitrageur does not face collateral losses and is willing to supply stablecoins at premia acceptable to a pessimistic speculator. In fact, the premium is zero when the speculator's demand for stablecoin is moderate (i.e., $\mu^s \in [\mu^{(1)}, 1)$) and does not exceed the arbitrageur's capital. If the speculator's demand is high ($\mu^s < \mu^{(1)}$), the arbitrageur charges a premium to dampen demand and satisfy the market-clearing condition. Note that the premium increases as μ^s decreases:

$$\frac{\partial p_D}{\partial \mu^s} = -\frac{1}{\left(\mu^s + \gamma\sigma_E^2\bar{\theta}W_0^a(\mu_E - \sigma_E)\right)^2} < 0. \tag{17}$$

The amount of stablecoin borrowing increases linearly as μ^s decreases until it reaches the arbitrageur's capital constraint.

Two key outcomes distinguish the case where $\mu_E < 1$ from the baseline $\mu^a \geq 1$. First, when $\mu^a < 1$, a no-trade region emerges for $\mu^s \in [\mu^{(2)}, \mu^{(3)}]$. The intuition mirrors the no-trade result from the rational expectations model, except that here the no-trade region is bounded. Its lower bound $\mu^{(2)}$ declines as μ^a decreases. Second, for $\mu^s \in [\mu^{(1)}, \mu^{(2)}]$—as the speculator's pessimism grows—trade occurs at a fixed price

$$p_D = 1 - \frac{\mu_E - 1}{\bar{\theta}(\mu_E - \sigma_E)},$$

rather than at $p_D = 1$, since the arbitrageur must now cover expected collateral losses. This price level, and the upper bound $\mu^{(2)}$, are independent of W_0^s, while the lower bound decreases with W_0^s. Hence, even if the arbitrageur's capital constraint is relaxed, the price premium is not eliminated. Panels A and B of Figure 2 illustrate comparative statics of p_D with respect to μ^s.

3.3 Introduction of Stable Collateral

In this section, we extend the model by allowing the arbitrageur to use a second stablecoin as collateral. We introduce a new stable collateral asset U (e.g., USDC) into the economy. As with asset E, the price p_U of asset U is taken to be exogenously given. The gross return on asset U, denoted R_U, is a random variable that takes the values $\mu_U + \sigma_U$ or $\mu_U - \sigma_U$ with probability 0.5 each, and is independent of R_E. Since U represents a stable collateral asset, we assume that $\sigma_U < \sigma_E$ and $\mu_U = 1$.

Furthermore, due to the lower risk of under-collateralization, the protocol allows for a higher maximum leverage constraint for stable collateral. Specifically, the collateral-dependent constraint $\bar{\theta}_U$ satisfies the condition:

$$\frac{\bar{\theta}_U}{\bar{\theta}} > \frac{\mu_E - \sigma_E}{1 - \sigma_U}. \tag{18}$$

This condition implies that liquidation risk is strictly lower when using stable collateral relative to risky collateral.

Proposition 2. When the arbitrageur can choose between risky and stable collateral, she always prefers the stable collateral. The equilibrium price and issuance of asset D are then determined by Equation (14), replacing μ^a with 1 and $(\mu_E - \sigma_E)$ with $(1 - \sigma_U)$ (see Equation (52) in Appendix B).

Proof: See Appendix B. An important implication of Proposition 2 is that the arbitrageur's trading strategy becomes independent of her beliefs about asset E. Moreover, when using stable collateral, the arbitrageur no longer faces expected collateral losses.

The introduction of stable collateral has several implications. Since the arbitrageur is no longer exposed to expected losses, and the stablecoin premium does not depend on the arbitrageur's beliefs or the type of collateral, the equilibrium price and borrowing behavior when $\mu^s > 1$ remain unchanged from the case with only risky collateral.

The key differences emerge when $\mu^s < 1$. In this case, the arbitrageur again avoids collateral losses, and the resulting equilibrium is similar to that under $\mu_E \geq 1$. However, stable collateral improves efficiency in three important ways. First, because liquidation risk is lower ($\sigma_U < \sigma_E$), the arbitrageur's capital constraint is relaxed. The threshold $\mu^{(1)}$ decreases, expanding the region where $p_D = 1$ and reducing the likelihood of large premia. Second, the protocol permits a higher leverage constraint $\bar{\theta}_U$ for stable collateral,

which further eases the capital constraint and enables more effective arbitrage. Third, the sensitivity of the stablecoin premium to μ^s declines, as shown by:

$$\frac{\partial p_D}{\partial \mu^s} = -\frac{1}{\left(\mu^s + \gamma\sigma_E^2\bar{\theta}_U W_0^a(1-\sigma_U)\right)^2} > -\frac{1}{\left(\mu^s + \gamma\sigma_E^2\bar{\theta} W_0^a(\mu_E-\sigma_E)\right)^2}, \tag{19}$$

whenever condition (18) holds.

Panel C of Figure 2 illustrates the comparative statics of p_D with respect to μ^s when arbitrageurs have access to stable collateral. Despite the reduction in premia and the improvement in arbitrage efficiency, stable collateral does not fully eliminate mispricing. Arbitrageurs still face the core friction of relying on future price convergence and committing scarce capital for a period of time to absorb speculative demand. This constraint is only fully resolved with the introduction of the PSM, which enables immediate, riskless arbitrage.

3.4 The Peg Stability Module

We now consider the introduction of the PSM, which allows traders to swap asset D for asset U at a fixed 1:1 rate at any time. This mechanism has a direct implication for the equilibrium price of D: the only possible equilibrium is $p_D = p_U$. Any deviation from this parity would create an arbitrage opportunity between D and U that is riskless and profitable. Since this arbitrage strategy has a Sharpe ratio approaching infinity, it dominates all speculative strategies involving asset E.

As a result, no other price of D is consistent with market clearing. Arbitrageurs will meet any excess supply or demand of D, whether it originates from leveraged long or short positions in asset E, provided they have sufficient capital.[15]

While the PSM effectively pegs D to U, it shifts the stability objective from maintaining parity with the US dollar to maintaining parity with another stablecoin. In practice, this means that the price of D now inherits any pricing deviations or stability concerns associated with U. If U trades below \$1, then D will also trade below 1. Therefore, price stability of D becomes entirely reliant on the robustness of U's peg.

This setup removes the influence of beliefs about asset E on the stablecoin price, but

15. This result assumes that the market for asset U is itself in equilibrium and that its price p_U reflects its fundamental value.

it does so by centralizing stability around the credibility of a single asset, U.

3.5 Empirical Predictions

Based on the theoretical results outlined above, we formulate the following hypotheses:

Determinants of DAI Borrowing

H1: *DAI borrowing by speculators increases, while DAI borrowing by arbitrageurs decreases, with the expected returns of risky cryptocurrencies.*

DAI Peg and Limits to Arbitrage

H2.1: *During the period when DAI is backed solely by risky collateral, DAI prices exhibit negative comovement with the expected returns of risky cryptocurrencies.*

H2.2: *Increased adoption of stable collateral types reduces limits to arbitrage, weakens the negative relationship between expected returns of risky cryptocurrencies and DAI prices, and improves peg efficiency.*

H2.3: *Greater adoption of PSM swaps further attenuates the negative effect of expected returns of risky cryptocurrencies on DAI prices and anchors the DAI price to USDC, increasing the correlation between DAI and USDC.*

4 Data

CDP Transaction-Level Data. To analyze the effects of collateral returns on investor borrowing behavior, we use the complete transaction history of MakerDAO's multi-collateral DAI (MCD) system, available online via MakerExplorer.[16] The dataset contains detailed records of every transaction made by individual CDPs, including the amount of collateral deposited, DAI borrowed, liquidation events, and precise timestamps. The sample spans from 18 November 2019 to 16 September 2024 and includes a total of 30,875 active CDPs.

Active CDPs are defined as positions that incurred a positive amount of DAI debt at any point in their lifetime. Table 1 provides a breakdown of these CDPs by collateral

16. Transaction-level data is sourced from DeFi Explorer: maker.defiexplore.com.

asset type, along with the number and percentage of CDPs that were liquidated. Among these, 19,562 CDPs are backed by ETH collateral, while 1,090 CDPs are backed by the stablecoin USDC. Other risky collateral types and stablecoins are also used. Among the alternative risky collateral types, Wrapped Bitcoin (WBTC) and wrapped staked Ether (wstETH) are the most common, with 3,116 and 1,062 CDPs respectively. Among alternative stablecoins, TrueUSD (TUSD) and Tether (USDT) are the most widely used, with 58 and 26 CDPs respectively.

The likelihood of liquidation varies significantly by collateral type. While only 6.45% of ETH-backed CDPs have experienced at least one liquidation event, more than half (51.56%) of USDC-backed CDPs have been liquidated at least once. The heightened exposure to liquidation risk for stablecoin vault users contributed to the launch of the PSM in December 2020.

For each CDP, we observe the key transaction actions such as transactions involving collateral (opening and closing a vault, depositing and withdrawing collateral, and transferring ownership across digital wallets), transactions involving DAI (borrowing and redeeming DAI tokens) and liquidations (when a vault becomes undercollateralized, a liquidation is triggered and the system liquidates the collateral to repay the DAI loan). This allows us to trace ETH collateral deposits, DAI borrowings, and redemptions over time and, as a result, to compute a real-time leverage ratio.

Table 2 summarizes key statistics for individual CDPs backed by ETH collateral (Panel A) and USDC collateral (Panel B), including the dollar value of DAI borrowing, collateral holdings, leverage ratios, and the number of liquidation events. For each CDP i at time t, we compute the stock of ETH collateral ($ETH_{i,t}$) and DAI borrowings ($DAI_{i,t}$), and apply the respective US dollar prices ($P_{ETH,t}$ and $P_{DAI,t}$) to evaluate their US dollar values.

ETH-backed CDPs (Panel A) display an average leverage ratio of 39%, well below the liquidation threshold of 66.67%. These CDPs borrowed an average maximum of 0.51 million DAI, with the largest CDP borrowing up to 1.5 billion DAI. Collateral holdings in ETH remain small on average (mean of 0.01 million ETH), and the average number of liquidations per ETH CDP is 0.07, with the maximum being 3.

In contrast, USDC-backed CDPs (Panel B) exhibit significantly higher leverage ratios, averaging 81%, with many CDPs operating close to the maximum allowed ratio of 99%. These CDPs borrow an average maximum of 0.95 million DAI, with the largest borrowing

reaching 72.9 million. The average collateral size is 0.99 million USDC, with a maximum of 75 million. USDC CDPs also experience more frequent liquidations: the average CDP is liquidated 0.70 times, with a maximum of 11 liquidation events.

Figure 3 complements these summary statistics by illustrating the distribution of leverage ratios for ETH and USDC CDPs. Panel A plots the kernel density of leverage ratios for ETH-backed CDPs, which are concentrated around 40%, with relatively little mass near the maximum ratio. In contrast, Panel B shows that USDC-backed CDPs tend to cluster near the upper limit of 100%, indicating that users borrowing against USDC collateral typically operate at much higher leverage. This pattern highlights the different risk management incentives and collateral profiles of users who borrow against stablecoins versus those who borrow against volatile assets like ETH. In our empirical evidence, we expand on this segmentation in the market and show that the motivations of these agents are different. While ETH-based collateral users typically borrowing DAI to speculate and take long leveraged positions in ETH. In contrast, the borrowing of DAI through stablecoin collateral is facilitating arbitrage.

Aggregate MakerDAO Data and Blockchain Network Measures. Data on aggregate system parameters—such as the DSR and total DAI issuance by collateral type (risky assets, stablecoins, real-world assets)—are sourced from MakerBurn.[17] This dataset also reports protocol policy settings such as stability fees and debt ceilings.

We complement this with blockchain-level network metrics from Coin Metrics, a provider of high-quality, standardized crypto-asset data. We use two measures: (i) *transactional value*, which captures the USD value of transfers between distinct addresses, and (ii) *velocity*, defined as the ratio of trailing one-year transaction volume to current supply. Velocity captures token turnover and serves as a proxy for DAI's usage intensity as a medium of exchange. Both metrics are used to track evolving demand for DAI in secondary markets and assess how it interacts with issuance behavior and peg dynamics.

Figure 4 provides an overview of key system indicators in the MakerDAO ecosystem. Panel A plots the DAI/USD price on Bitfinex, the earliest exchange with reliable trading data, and illustrates persistent but time-varying deviations from the 1 USD peg. On average, DAI traded at a premium of 100 basis points during the pre-PSM sample period. This premium compressed substantially in the post-PSM period, averaging just 2.4 basis

17. Available at makerburn.com.

points. Panel B shows the evolution of two key policy instruments—the DSR and the ETH Stability Fee. While stability fees reached highs of 20% in 2019, the average borrowing rate over the full period is approximately 3%. Panel C displays the total supply of DAI disaggregated by collateral type: risky crypto assets (e.g., ETH, WBTC), stablecoins (e.g., USDC in CDP vaults or through the PSM), and real-world assets (RWA). Panel D presents daily ETH liquidation volumes, highlighting significant spikes during stress events such as March 12, 2020, when ETH declined by over 50% in a single day. Despite high market volatility, the system maintains relatively conservative leverage in response to liquidation risk: the average loan-to-value ratio for ETH collateral is approximately 39%, well below the maximum allowable leverage of 66%.

Spot and Futures Price Data. We obtain spot price data for ETH, DAI, and other collateral assets from the *CoinDesk Digital Asset Data API*, a proprietary platform offering high-frequency data across major cryptocurrency exchanges.[18] Where multiple exchanges provide similar coverage, we prioritize those (i) with the longest continuous time series and (ii) designated as "trusted volume" exchanges by the SEC, based on assessments of market integrity.[19] The SEC report evaluates exchanges for signs of market manipulation, such as irregular bid-ask spreads or clustered trade sizes.

For ETH/USD and DAI/USD spot prices, we use data from the Coinbase and Bitfinex exchanges, respectively. USDC/USD prices are sourced from Kraken, while DAI/USDC prices are from Coinbase. We compute intra-day volatility as the square root of the sum of squared 5-minute returns within each trading day.

For futures markets, we use perpetual futures data from Binance, covering ETH-USDT and BTC-USDT pairs. Alongside the data on the futures price, we incorporate associated funding rates to proxy forward-looking return expectations in the derivatives market.

Proxies of Expected Returns of Risky Cryptocurrencies. We construct two distinct proxies for speculators' expected ETH returns: one based on perpetual futures market pricing, and another derived from investor sentiment. Both proxies are standardized prior to inclusion in our empirical analysis.

Perpetual futures-based proxy. Our primary market-based proxy is constructed from pricing data in the perpetual futures market. Perpetual futures are derivative contracts

18. See the CoinDesk Data API Documentation.
19. See the SEC comment letter on NYSE Arca 2019-01.

without expiration, relying on periodic funding payments to maintain price alignment with the underlying spot asset. Perpetual futures has been used as a measure of cryptocurrency sentiment and in constructing expected returns in the cryptocurrency market (Gorton et al., 2022; Chaudhary, Kozhan, and Viswanath-Natraj, 2023; Capponi and Ramesh, 2024). The expected return from holding a long position in perpetual futures reflects two components: the daily futures price premium and the cost (or rebate) from funding payments.

The expected return from a long perpetual position should equal the expected return from holding the cryptocurrency in the spot market. This leads us to define the following daily return proxy:

$$\mathbb{E}[R^k_{\text{perp},t}] = \left(\frac{\overline{P}^{\text{fut}}_t}{P^{\text{spot}}_{t-1}} - 1 \right) - \text{funding payment},$$

where $\overline{P}^{\text{fut}}_t$ denotes the intraday (hourly) average of the perpetual futures price for currency k on day t, and P^{spot}_{t-1} is the lagged spot price. The funding payment represents the daily sum of compound interest accrued from funding rates applied every 8 hours.[20] This proxy captures the net economic incentive to hold long positions in perpetual futures and incorporates forward-looking return expectations implied by derivatives markets.

Sentiment-based proxy. For a measure of investor sentiment, we use the standardized value of the *Crypto Fear and Greed Index*, which aggregates sentiment signals across several public sources. The index ranges from 0 ("Extreme Fear") to 100 ("Extreme Greed") and is composed of five weighted inputs: volatility (25%), market momentum and volume (25%), social media trends (15%), market dominance (10%), and Google Trends (10%).[21]

Table 3 provides summary statistics for variables used in the analysis. This includes the DAI price, ETH returns as well as system parameters such as interest rates and the market cap over our sample period from November 18, 2019 to December 31, 2024.

20. For daily returns, we approximate the funding payment as $3 \times \overline{\text{funding rate}}$, where $\overline{\text{funding rate}}$ is the intraday (hourly) average.

21. The index is available via an API at alternative.me/crypto/fear-and-greed-index.

5 Empirical evidence

5.1 CDP Data: Speculators and Arbitrageurs

5.1.1 A Case Study

To build intuition around speculative versus arbitrage-driven borrowing in the MakerDAO system, Figure 5 presents time series plots for two representative CDPs.

Panel A shows CDP #8463, an illustrative case of speculative borrowing. The vault is collateralized with ETH and displays leveraged trading behavior: DAI debt levels closely track the USD value of the collateral. The leverage ratio remains elevated and responds dynamically to ETH price movements. These patterns suggest the user is engaging in directional bets, increasing DAI borrowing when prices rise and scaling back during downturns—consistent with speculative motives.

Panel B displays CDP #10775, backed by USDC, and illustrates behavior consistent with arbitrage. Borrowing patterns are relatively flat and insensitive to collateral price movements, suggesting the vault owner may be minting DAI to exploit pricing discrepancies – when DAI trades at a premium to USD – rather than pursuing speculative returns.

5.1.2 Determinants of DAI Borrowing

To formally test Hypothesis 1 – that DAI borrowing is responsive to speculative return expectations – we estimate the following panel regression:

$$Y_{i,t} = \alpha_i + \beta_1 \mathbb{E}_t[\tilde{R}^{ETH}] + \beta_2 (p_t^{DAI} - 1) + \text{Controls}_t + u_{i,t}, \tag{20}$$

where $Y_{i,t}$ denotes the change in outstanding DAI debt (in millions) for vault i at time t, and $\mathbb{E}_t[\tilde{R}^{ETH}]$ represents either realized ETH returns, perpetual futures-implied returns, or sentiment-based forecasts. The variable $(p_t^{DAI} - 1)$ captures peg-price deviations. All regressions include CDP fixed effects and instrument the peg deviation using its own lag and the ETH realized return, along with ETH volatility and lags of the DAI Stability Fee and vault-specific borrowing fees.

We estimate Equation (20) separately for CDPs collateralized with ETH and USDC to distinguish speculative from arbitrage-motivated borrowing.

ETH-Backed CDPs. Table 4 presents results for CDPs using ETH as collateral. Columns (1) through (4) show that expected ETH returns are strong and significant predictors of DAI borrowing. In particular, the futures-implied return proxy is positively associated with borrowing ($\beta_1 = 0.0500$, $p < 0.01$), and the sentiment-based proxy is also significant ($\beta_1 = 0.0969$, $p < 0.05$). These results confirm that bullish return expectations incentivize speculative leveraging among ETH-backed borrowers.

Peg-price deviations ($p_t^{DAI} - 1$) are also positively and significantly associated with ETH CDP borrowing across specifications. This suggests that speculators not only respond to expected ETH returns but also account for the effective cost of implementing strategies using DAI. That is, when DAI trades above its peg, borrowing becomes more attractive, amplifying issuance. The peg deviation term is instrumented using its own lag and ETH return, along with ETH volatility and lagged policy rates. The instrument set is strong: the first-stage F-statistic from a time-series regression of the DAI price on these instruments is 1000.88, well above conventional thresholds.

Our theoretical results motivate us to use proxies of expected ETH returns reflecting sentiments in the market in line with the heterogeneous beliefs version of the model rather than the rational expectations. To test for this prediction, we also include the realized return as a proxy for unbiased expectation of ETH return along with our two proxies of expected ETH return. The result shows that the proxies of speculator's expected returns remain negative and statistically significant while the realized returns variable is significant only in one specification and with a coefficient more than twice smaller than the sentiment-based proxy. The realized return could control for an effect of unexpected return on DAI borrowing.

Taken together, the ETH CDP results support Hypothesis 1: speculative behavior drives DAI borrowing, and such borrowing responds to both return expectations and secondary market pricing.

USDC-Backed CDPs. Table 5 shows results for CDPs using USDC collateral. We reject the hypothesis that expected ETH return is unrelated to DAI borrowing in the specification with the sentiment-based proxy ($\beta_1 = -0.276$, $p < 0.05$). This result is consistent with Hypothesis 1 and the model prediction: during bearish ETH episodes (when sentiment is strongly negative), arbitrageurs step in to meet increased DAI demand from short sellers and deleveraging speculators. This results in a countercyclical supply

response by arbitrageurs, in contrast to speculators that borrow DAI in periods of high expected returns. We do not reject the hypothesis when the proxy based on perpetual futures is used.

Interestingly, peg deviations no longer significantly predict borrowing in these USDC-backed CDPs. This finding differs from earlier specifications using ETH CDPs and suggests that arbitrage is not significant linked to peg-price deviations. Similarly, the realized return proxy is insignificant in both specifications suggesting that it is the speculators beliefs driving DAI borrowing.

Overall, the panel evidence validates hypothesis H1: ETH-based borrowing is driven by speculative expectations and peg conditions, while USDC-based borrowing reflects a more stable, countercyclical response consistent with arbitrage.

5.2 Limits to Arbitrage and Collateral Returns

5.2.1 A Case Study

To motivate the effect of collateral risk on DAI prices, we analyze three historical episodes to illustrate the role of arbitrage design. Figure 6 presents case studies from March 2020, May 2021, and March 2023, each highlighting different aspects: limits to arbitrage under risky collateral, the role of the PSM in alleviating limits to arbitrage and compressing peg premiums, and the role of the PSM in determining peg discounts of USDC.

Panel A of Figure 6 focuses on the March 12, 2020 "Black Thursday" crash – an extreme ETH return shock during the single-collateral DAI regime. DAI traded at significant premiums, spiking to approximately 8% premiums. Consistent with a negative shock to ETH returns, risky collateral-backed borrowing plummeted, and DAI supply contracted sharply, revealing the fragility of the peg when arbitrage relies entirely on volatile collateral such as ETH. Interestingly, the MakerDAO protocol decided to add USDC as a collateral type shortly after this event on March 12, 2020, and we begin to see a small increase in USDC-backed DAI borrowing in the days after the crash.

Panel B shows the response to a similar ETH price crash on May 19, 2021. While ETH again experienced steep losses, DAI premiums remained limited to 40–50 basis points. The crypto-backed DAI supply fell in response to rising liquidations and collateral losses, but was offset by an increase in PSM-based issuance. This pattern reflects improved peg stability via the PSM, which relaxed arbitrage constraints by enabling stablecoin-

backed DAI issuance. Comparing this episode to the prior case in panel A how the PSM compresses peg deviations during episodes of negative ETH returns, when arbitrageurs may otherwise face binding constraints due to risky collateral.

While Panel B illustrates the positive aspects of the PSM, Panel C turns to a contrasting scenario: the March 2023 de-pegging of USDC following the collapse of Silicon Valley Bank (SVB), where Circle, the issuer of USDC, held $3.3 billion in reserves. As investor confidence in USDC fell, both USDC and DAI dropped to as low as $0.87 on March 11. In this instance, DAI became anchored to USDC via the PSM, which linked DAI supply directly to USDC inflows. Arbitrageurs used the PSM to stabilize the DAI/USDC rate at 1:1, but this also meant DAI inherited the devaluation of USDC. The episode illustrates a key trade-off: while the PSM enhances peg efficiency under ETH volatility, it introduces fragility when the anchor asset—USDC—comes under stress.

Following this event, MakerDAO governance sought to reduce exposure to USDC by diversifying its reserves. In March 2023, Maker increased its U.S. Treasury holdings from $750 million to $1.25 billion, reallocating $500 million in PSM-held USDC.[22] This shift highlights an important implication: peg design via the PSM introduces a dependence on the integrity of the anchor asset, which – if compromised – can propagate instability to DAI itself.

5.2.2 DAI Price and expected ETH Return: Contemporaneous Regressions

This section formally tests whether the adoption of stable collateral mitigates limits to arbitrage for the DAI stablecoin. Specifically, we examine the contemporaneous relationship between DAI peg-price deviations and ETH return shocks using the following regression specification:

$$p_t^{DAI} - 1 = \alpha + \beta_1 \mathbb{E}_t[\tilde{R}^{ETH}] + \beta_2 \mathbb{E}_t[\tilde{R}^{ETH}] \times \text{Share Safe}_t + \text{Controls}_t + \varepsilon_t, \tag{21}$$

where $p_t^{DAI} - 1$ denotes the basis point deviation of the DAI price from its 1 USD peg, and $\mathbb{E}_t[\tilde{R}^{ETH}]$ is a standardized ETH return proxy. In this analysis, we focus on two proxies: the forward-looking perpetual futures return $\mathbb{E}_t[\tilde{R}^{\text{ETH}}_{\text{perp}}]$ and a sentiment-based return proxy $\mathbb{E}_t[\tilde{R}^{\text{ETH}}_{\text{sent}}]$. The variable Share Safe_t measures the share of DAI backed by fiat-backed stablecoins such as USDC. We exclude DAI backed by RWA to ensure this

22. See: twitter.com/MakerDAO/status/1636423561941327873.

variable captures liquid, on-chain arbitrage capacity.

We interpret Share Safe$_t$ as a continuous proxy for arbitrage constraints: higher values indicate greater capacity for frictionless arbitrage. Figure 7, Panel A, shows its evolution, with sharp increases following two major events: (i) the addition of USDC as eligible collateral in March 2020 and (ii) the launch of the PSM in December 2020, which enabled 1:1 USDC–DAI swaps without vault creation.

Under Hypotheses H2.1–H2.3, we assess how the impact of expected ETH return on DAI prices varies across collateral regimes. When Share Safe$_t$ $= 0$, the system is fully backed by risky collateral, and limits to arbitrage are severe. In this regime, the coefficient β_1 captures the sensitivity of the peg to ETH return shocks. We expect $\beta_1 < 0$, consistent with H2.1: as ETH appreciates, leveraged CDP borrowing increases DAI issuance, lowering the DAI price; during downturns, CDPs deleverage, raising the price.

The interaction coefficient β_2 captures how the ETH–DAI relationship evolves as stable collateral is adopted. Higher Share Safe$_t$ lowers barriers to arbitrage by allowing direct DAI issuance or redemption. We therefore expect $\beta_2 > 0$, consistent with H2.2 and H2.3: safe collateral dampens the effect of ETH return shocks on the peg.

Table 6 presents instrumental variable (IV) estimates of DAI peg-price deviations in response to ETH return proxies, their interaction with the share of safe collateral, and indicators for extreme return events. Two variables—ETH liquidations and a proxy for DAI demand (velocity)—are treated as endogenous and instrumented using their own lags as well as lagged protocol rates: the DSR and the ETH Stability Fee. All regressions control for lagged peg deviations and ETH volatility.

Column (1) uses the perpetual futures return proxy. The coefficient is negative and statistically significant ($\beta_1 = -0.178$, $p < 0.05$), consistent with H2.1: speculative return shocks are associated with deviations from the DAI peg. The interaction term is positive and significant ($\beta_2 = 0.381$, $p < 0.05$), supporting H2.2—namely, that as the share of safe collateral increases, arbitrage activity becomes more effective and dampens the impact of return shocks.

Column (2) replaces the futures proxy with a sentiment-based return measure. Again, the estimated return effect is negative ($\beta_1 = -0.072$, $p < 0.05$), and the interaction with the share of safe collateral is positive and significant ($\beta_2 = 0.166$, $p < 0.05$), indicating that expectation-driven movements in ETH returns also influence the peg but are more

muted in safer collateral environments.

Columns (3) and (4) include nonlinear terms for extreme negative return episodes. In Column (3), a dummy for perpetual return crashes ($< -2\sigma$) is positive (0.549), consistent with large upward peg deviations during ETH selloffs. The interaction term is negative (-2.100), suggesting that higher adoption of safe collateral attenuates the peg's sensitivity to such events, although the coefficient is not statistically significant. Column (4) considers extreme sentiment shocks ($< -1.5\sigma$). Both the dummy (0.446, $p < 0.1$) and the interaction term (-0.841, $p < 0.1$) are weakly significant, indicating that while severe sentiment-driven downturns elevate the peg, their effect is substantially reduced in safer regimes.

Across all columns, lagged peg deviations are large and highly significant, indicating persistent deviations and slow mean reversion. The share of safe collateral is consistently negative and significant, confirming its stabilizing role independent of return shocks.

The instruments for ETH liquidations and DAI velocity are relevant. The Sanderson-Windmeijer first-stage F-statistic for velocity exceeds 130,000, while the corresponding value for liquidations is 6.80. These values exceed conventional thresholds for weak identification, supporting the strength of the instrument set.

Overall, the evidence supports H2.1 and H2.2: return shocks—particularly those tied to speculation or sentiment—are negatively correlated with peg prices peg in regimes with constrained arbitrage. Access to safe collateral types (e.g., via the PSM) significantly mitigates these effects.

5.2.3 DAI Price and expected ETH Return: Dynamic Effects

A key empirical concern in our baseline regressions is the potential endogeneity of explanatory variables—such as liquidations, secondary market demand, and protocol rates—with respect to DAI price movements. For example, a peg deviation may trigger liquidations or influence on-chain trading activity, rather than merely result from them. To address this simultaneity, we estimate a Structural Vector Autoregression (SVAR) model, which accommodates feedback effects and contemporaneous interactions among key variables affecting the DAI peg.

Our identification strategy follows recent work on price formation in decentralized markets (Capponi, Jia, and Yu, 2022; Klein et al., 2023) and macro-financial dynamics in

crypto ecosystems (Adams, Ibert, and Liao, 2024). The SVAR specification is given by:

$$AY_t = A_0 + \sum_{j=1}^{N} A_j Y_{t-j} + \Gamma Z_t + \epsilon_t, \tag{22}$$

where Y_t is a vector of endogenous variables, ordered as:

$$Y_t = \left[\mathbb{E}_t[\tilde{R}^{\text{ETH}}],\ \text{Fee}_t,\ \text{DSR}_t,\ \text{Liq}_t,\ \log(\text{Supply}_t),\ \log(\text{Demand}_t),\ p_t^{\text{DAI}} - 1\right]',$$

and ϵ_t is a vector of orthogonal structural shocks. Here, $\mathbb{E}_t[\tilde{R}^{\text{ETH}}]$ denotes the ETH return proxy (using the perpetual funding rate as the baseline specification), Fee_t is the ETH collateral stability fee, DSR_t is the DAI Savings Rate, Liq_t is the ETH collateral liquidation volume (in millions), $\log(\text{Supply}_t)$ is the log of circulating DAI supply, $\log(\text{Demand}_t)$ captures secondary market usage on the blockchain, and $p_t^{\text{DAI}} - 1$ is the DAI peg deviation.

The vector Z_t includes exogenous controls that condition the dynamic system. Specifically, Z_t comprises the share of DAI backed by safe collateral (Share Safe_t), along with the interaction term $\mathbb{E}_t[\tilde{R}^{\text{ETH}}] \times \text{Share Safe}_t$. These allow us to isolate the effect of ETH return and liquidation shocks under regimes where DAI is primarily backed by risky collateral (i.e., when $\text{Share Safe}_t = 0$). This is important, as the growth of safe collateral over time may otherwise confound the estimated impulse responses.

The reduced-form VAR is written as:

$$Y_t = C_0 + CY_{t-1} + \Phi Z_t + B\epsilon_t, \tag{23}$$

where $B = A^{-1}$, $C = A^{-1}A_1$, and $\Phi = A^{-1}\Gamma$. Identification uses a recursive (Cholesky) ordering in which ETH returns are contemporaneously exogenous, while DAI price deviations may respond immediately to all other variables. This reflects the view that ETH shocks originate externally, while peg deviations reflect endogenous MakerDAO responses.

The SVAR is estimated with $N = 5$ lags. Impulse response functions (IRFs) are computed using 1,000 wild bootstrap replications. Solid lines show point estimates; shaded regions are 95% confidence intervals.

Figure 8 presents the impulse response functions (IRFs) following a one-standard-deviation shock to the ETH return, proxied by the perpetual funding rate. Panel A shows a significant and persistent decline in the DAI price, with a cumulative effect of

approximately 1.5 percentage points. This supports our hypothesis that rising expected ETH returns increase CDP borrowing and DAI issuance, placing downward pressure on the peg.

Panels B and C display the effects of the Stability Fee and the DAI Savings Rate (DSR), respectively. A one-percentage-point increase in the DSR raises the DAI price—albeit modestly—by roughly 2–3 percentage points over a three-month horizon. This suggests that the DSR acts as a monetary tightening tool by incentivizing users to lock up DAI. In contrast, the Stability Fee has no significant effect, indicating that collateral-based rates are less effective in managing the peg in real time.[23]

Panel D illustrates the short-run impact of liquidations. The DAI price rises briefly—possibly due to liquidation-induced demand for DAI—but the effect is transitory. The muted long-run response likely reflects the limited systemic scale of MakerDAO liquidations, which are too small to trigger feedback loops or fire sales, consistent with Lehar and Parlour, 2022.

Panels E and F assess the supply and demand channels. The response to DAI supply is strongly negative: higher issuance pushes the price below parity. The estimates imply that a 1% increase in aggregate DAI issuance lowers the DAI price by approximately 0.4 percentage points. By contrast, the demand proxy—measured by on-chain transfer value of DAI—has only a weak and delayed positive effect. A 1% increase in demand raises the DAI price by about 0.5 basis points. The weak effects are likely due to the inclusion of non-demand-related transfers in the volume metric.

In sum, the SVAR results reinforce our earlier findings. Under a risky collateral regime, DAI price deviations exhibit a strong and negative co-movement with expected ETH return shocks. These results remain robust after accounting for endogenous policy rates, macro-financial fundamentals, and feedback effects captured within the SVAR framework.

5.2.4 Limits to Arbitrage and Peg Efficiency

This section investigates whether the adoption of stable collateral—particularly through the PSM—reduces limits to arbitrage and improves peg efficiency. The outcome variable is the absolute peg deviation $|p_t^{DAI} - 1|$, which captures the extent to which the DAI price

23. See Sun, Stasinakis, and Sermpinis, 2024 for a discussion of governance concentration, voter incentives, and the resulting frictions limiting the responsiveness of protocol parameters.

departs from its USD peg. Table 7 reports OLS estimates of the following regression:

$$|p_t^{DAI} - 1| = \alpha + \beta_1 \text{ShareSafe}_t^{(i)} + \beta_2 \text{ShareSafe}_t^{(i)} \times \mathbf{1}\{p_t^{DAI} > 1\} + \text{Controls}_t + \varepsilon_t, \quad (24)$$

where $\text{ShareSafe}_t^{(i)}$ denotes the share of DAI backed by safe collateral—either aggregated, vault-based (e.g., USDC), or issued through the PSM. Controls include ETH volatility, the DAI Stability Fee, ETH liquidations, and a proxy for transactional demand (DAI velocity). Standard errors are robust to heteroscedasticity. The sample spans from November 18, 2019 to September 16, 2024.

Column (1) includes only the aggregate share of safe collateral. A 1% increase in the safe collateral share reduces the absolute peg deviation by 0.3 basis points ($\beta_1 = -0.302$, $p < 0.01$), indicating that safer collateral improves peg stability. This supports Hypothesis H2.2, which posits that collateral stability lowers arbitrage frictions.

Column (2) disaggregates the safe share into vault-based and PSM-based collateral. The coefficient on the PSM share is -0.312 ($p < 0.01$), while the USDC vault share is statistically insignificant. This finding suggests that the PSM—by enabling frictionless, on-chain swaps at a fixed 1:1 price—is a more effective arbitrage design than vault-based issuance, which remains subject to liquidation constraints. This supports Hypothesis H2.3.

Column (3) examines asymmetries in arbitrage effectiveness by interacting the aggregate safe share with an indicator for positive peg deviations ($\mathbf{1}\{p_t^{DAI} > 1\}$). The interaction term is negative and significant ($\beta_2 = -0.229$, $p < 0.01$), while the indicator itself is positively signed ($\beta = 0.156$, $p < 0.01$). This indicates that safe collateral, particularly via the PSM, is especially effective at compressing peg-price deviations when DAI trades above 1.00. In line with H2.3, the presence of the PSM enhances mean reversion dynamics and reinforces the peg.

Taken together, these results demonstrate that DAI's peg efficiency improves significantly with the adoption of safe collateral, and even more so when that collateral is intermediated through the PSM. The findings highlight that arbitrage mechanism design matters: while decentralized collateral like ETH enables a censorship-resistant stablecoin, it introduces price volatility that limits arbitrage efficiency. The PSM, by anchoring DAI to a centralized stablecoin and enabling frictionless arbitrage, appears necessary to overcome those constraints and compress peg premiums.

5.3 Robustness Tests

CDP Tests. Appendix C presents several robustness checks on CDP-level borrowing behavior. Table A1 splits the sample by user activity and shows that CDPs with higher transaction frequency respond more strongly to ETH return signals and peg deviations—consistent with more sophisticated, speculative strategies.

Table A2 explores nonlinearities in borrowing responses to ETH returns by interacting return proxies with indicators for extreme negative episodes. Results for the perpetual futures proxy show a significantly negative interaction term, indicating that the relationship between expected returns and borrowing weakens—i.e., becomes less elastic—when returns fall below -2σ. This attenuation is consistent with constrained risk-taking during stress periods. Sentiment-based proxies show similar directional patterns, though the interaction effects are less precisely estimated.

Finally, Table A3 confirms that CDPs using WBTC collateral behave similarly to those using ETH, with borrowing increasing in response to expected BTC returns.

DAI Price and Expected ETH returns: Dynamic Effects. Appendix D reports IRFs from an alternative SVAR specification where ETH return shocks are measured using a sentiment-based proxy instead of perpetual futures. Figure A4 shows that the dynamic response of DAI prices remains consistent: ETH return shocks trigger negative price effects, while monetary policy instruments (such as the DSR) help stabilize the peg. This robustness confirms that the negative comovement between DAI prices and ETH returns holds across different return measures.

Peg Efficiency. Appendix E presents additional tests of peg stability. Table A4 shows that the introduction of safe collateral—especially via the PSM—significantly reduces intra-day DAI price volatility. A one-unit increase in the safe collateral share reduces volatility by over 40 basis points, and the effect is stronger for PSM-backed DAI than for vault-based USDC. Furthermore, interaction terms with ETH volatility confirm that safe collateral dampens the pass-through of collateral market volatility to the DAI peg.

Table A5 estimates a Self-Exciting Threshold AutoRegressive (SETAR) model and finds that the band of inaction around the DAI peg compresses after the PSM's introduction—from $[-8, 287]$ basis points pre-PSM to $[1, 27]$ basis points post-PSM. Additionally, the half-life of large peg premiums falls from 2.51 to 0.78 days. These results confirm

that the PSM facilitates faster mean reversion and tighter arbitrage bounds by providing a scalable issuance channel for stabilizing trades.

6 Conclusion

This paper examines the determinants of DAI's peg stability, focusing on the role of speculative behavior and limits to arbitrage. Using CDP-level data, we show that speculative borrowing, driven by expectations of ETH returns, exerts significant pressure on the DAI price. These effects are particularly strong when DAI is backed predominantly by volatile crypto collateral, and they persist even after accounting for liquidations and demand-side forces.

Arbitrage activity helps offset these pressures but is constrained by collateral risk and the absence of a direct conversion mechanism between DAI and safe assets. The introduction of stable collateral, such as USDC, alleviates some of these constraints by reducing exposure to expected losses and liquidation risk. Peg efficiency improves further after the launch of the PSM, which enables 1:1 swaps between DAI and USDC. This closes arbitrage gaps in real time but increases reliance on centralized stablecoins and their underlying reserves.

Our findings highlight a core design tension in decentralized stablecoins. Systems backed solely by crypto collateral preserve decentralization but restrict arbitrage capacity and expose the peg to speculative dynamics. Incorporating stable collateral improves peg stability but introduces re-centralization and dependence on custodial assets. An efficient stablecoin design therefore requires balancing decentralization with the efficiency and reliability of arbitrage mechanisms.

Future Work. Our findings offer broader implications for the design and regulation of stablecoins. While our analysis centers on DAI, other stablecoins—such as USDC and Tether—face distinct risks, including custodial exposure and redemption frictions. A key challenge for decentralized stablecoins is balancing the use of risky crypto collateral with the benefits and risks of incorporating centralized assets.

Looking ahead, a promising direction is to model optimal arbitrage design in settings where stablecoins compete along dimensions of decentralization, liquidity, and stability. Formal models of arbitrage under collateral risk and governance frictions could

help clarify the costs and benefits of direct redemption mechanisms like the PSM. As new entrants—such as tokenized bank deposits and central bank digital currencies (CBDCs)—emerge, decentralized stablecoins will need to adapt. Tokenized fiat, particularly when issued by central banks, may offer a stable collateral layer that reduces reliance on custodians without undermining on-chain settlement. The long-term viability of decentralized money will depend on how effectively such innovations can be integrated into future stablecoin architectures.

References

Adams, Austin, Markus Ibert, and Gordon Liao. 2024. "What Drives Crypto Asset Prices?" *Available at SSRN.*

Arner, Douglas W, Raphael Auer, and Jon Frost. 2020. "Stablecoins: Risks, Potential and Regulation." *Financial Stability Review. Nº 39 (Autumm 2020), p. 95-123.*

Barthelemy, Jean, Paul Gardin, and Benoît Nguyen. 2021. "Stablecoins and the Real Economy." *Available at SSRN 3973538.*

Bertsch, Christoph. 2023. "Stablecoins: Adoption and Fragility."

Borri, Nicola, and Kirill Shakhnov. 2018. "Cryptomarket Discounts." *Available at SSRN 3124394.*

Brunnermeier, Markus K, and Lasse Heje Pedersen. 2009. "Market Liquidity and Funding Liquidity." *The review of financial studies* 22 (6): 2201–2238.

Capponi, Agostino. 2024. *The Evolution of DeFi: Achievements, Challenges, and the Road Ahead.* Presented at the Shard Annual Conference 2024, Warwick Business School, September. https://warwick.ac.uk/fac/soc/wbs/subjects/finance/gillmore/annualconference2024agenda/11.00_agostino_warwick_latest.pdf.

Capponi, Agostino, Ruizhe Jia, and Shihao Yu. 2022. "The Information Content of Blockchain Fees." *Available at SSRN.*

Capponi, Agostino, and Sathya Ramesh. 2024. "Predictable Booms and Busts in Cryptocurrency: Evidence from Perpetual Futures." Working paper. https://papers.ssrn.com/sol3/papers.cfm?abstract_id=4091581.

Chappell, David, Joanne Padmore, Priti Mistry, and Catherine Ellis. 1996. "A threshold model for the French franc/Deutschmark exchange rate." *Journal of Forecasting* 15 (3): 155–164.

Chaudhary, Amit, Roman Kozhan, and Ganesh Viswanath-Natraj. 2023. "Interest Rate Parity in Decentralized Finance." *WBS Finance Group Research Paper Forthcoming.*

Chiu, Jonathan, Emre Ozdenoren, Kathy Yuan, and Shengxing Zhang. 2022. "The Fragility of DeFi Lending."

Clements, Michael P, and Jeremy Smith. 2001. "Evaluating Forecasts from SETAR Models of Exchange Rates." *Journal of International Money and Finance* 20 (1): 133–148.

d'Avernas, Adrien, Thomas Bourany, and Quentin Vandeweyer. 2022. "Can Stablecoins be Stable?" *Working Paper.*

Dell'Erba, Marco. 2019. "Stable Cryptocurrencies? Assessing the Case for Stablecoins." *New York University Journal of Legislation and Public Policy, Forthcoming.*

Eichengreen, Barry, My Nguyen, and Ganesh Viswanath-Natraj. 2023. "Stablecoin Devaluation Risk." *WBS Finance Group Research Paper.*

Force, ECB, et al. 2020. *Stablecoins: Implications for Monetary Policy, Financial Stability, Market Infrastructure and Payments, and Banking Supervision in the Euro Area.* Technical report. European Central Bank.

Frost, Jon, Hyung Song Shin, and Peter Wierts. 2020. "An Early Stablecoin? The Bank of Amsterdam and the Governance of Money."

Gorton, Gary B, Elizabeth C Klee, Chase P Ross, Sharon Y Ross, and Alexandros P Vardoulakis. 2022. *Leverage and Stablecoin Pegs.* Technical report. National Bureau of Economic Research.

Gorton, Gary B, Chase P Ross, and Sharon Y Ross. 2022. *Making Money.* Technical report. National Bureau of Economic Research.

Gromb, Denis, and Dimitri Vayanos. 2002. "Equilibrium and Welfare in Markets with Financially Constrained Arbitrageurs." *Journal of financial Economics* 66 (2-3): 361–407.

———. 2018. "The Dynamics of Financially Constrained Arbitrage." *The Journal of Finance* 73 (4): 1713–1750.

Gu, Wanyun Catherine, Anika Raghuvanshi, and Dan Boneh. 2020. "Empirical Measurements on Pricing Oracles and Decentralized Governance for Stablecoins." *Available at SSRN 3611231.*

Gudgeon, Lewis, Sam Werner, Daniel Perez, and William J Knottenbelt. 2020. "DeFi Protocols for Loanable Funds: Interest Rates, Liquidity and Market Efficiency." In *Proceedings of the 2nd ACM Conference on Advances in Financial Technologies,* 92–112.

Hansen, Bruce. 1999. "Testing for Linearity." *Journal of Economic Surveys* 13 (5): 551–576.

Harvey, Campbell R, Ashwin Ramachandran, and Joey Santoro. 2021. *DeFi and the Future of Finance.* John Wiley & Sons.

Heimbach, Lioba, and Wenqian Huang. 2024. *Defi leverage.* Bank for International Settlements, Monetary / Economic Department.

Hoang, Lai T, and Dirk G Baur. 2020. "How Stable are Stablecoins?" *Available at SSRN 3519225.*

Hutchison, Michael M, Gurnain Kaur Pasricha, and Nirvikar Singh. 2012. "Effectiveness of capital controls in India: Evidence from the offshore NDF market." *IMF Economic Review* 60 (3): 395–438.

John, Kose, Leonid Kogan, and Fahad Saleh. 2023. "Smart contracts and decentralized finance." *Annual Review of Financial Economics* 15 (1): 523–542.

Klages-Mundt, Ariah, and Andreea Minca. 2020. "While Stability Lasts: A Stochastic Model of Stablecoins." *arXiv preprint arXiv:2004.01304.*

Klein, Olga, Roman Kozhan, Ganesh Viswanath-Natraj, and Junxuan Wang. 2023. "Price Discovery in Cryptocurrencies: Trades versus Liquidity Provision." *Available at SSRN 4642411.*

Kozhan, Roman, and Ganesh Viswanath-Natraj. 2022. "Fundamentals of the MakerDAO Governance Token." In *3rd International Conference on Blockchain Economics, Security and Protocols (Tokenomics 2021).* Schloss Dagstuhl-Leibniz-Zentrum für Informatik.

Lehar, Alfred, and Christine A Parlour. 2022. "Systemic Fragility in Decentralized Markets."

Li, Ye, and Simon Mayer. 2020. "Managing Stablecoins: Optimal Strategies, Regulation, and Transaction Data as Productive Capital." *Fisher College of Business Working Paper,* nos. 2020-03: 030.

Lyons, Richard K, and Ganesh Viswanath-Natraj. 2023. "What Keeps Stablecoins Stable?" *Journal of International Money and Finance* 131:102777.

Ma, Yiming, Yao Zeng, and Anthony Lee Zhang. 2023. "Stablecoin Runs and the Centralization of Arbitrage." *Available at SSRN 4398546.*

Makarov, Igor, and Antoinette Schoar. 2019. "Price Discovery in Cryptocurrency Markets." In *AEA Papers and Proceedings,* 109:97–99.

———. 2020. "Trading and Arbitrage in Cryptocurrency Markets." *Journal of Financial Economics* 135 (2): 293–319.

Nyborg, Kjell G, and Cornelia Rösler. 2019. "Repo rates and the collateral spread: Evidence."

Oefele, Nico, Dirk G Baur, and Lee A Smales. 2024. "Are stablecoins the money market mutual funds of the future?" *Journal of Empirical Finance* 79:101557.

Perez, Daniel, Sam M Werner, Jiahua Xu, and Benjamin Livshits. 2020. "Liquidations: DeFi on a Knife-edge." *arXiv preprint arXiv:2009.13235.*

Pernice, Ingolf, and Gunnar Anton. 2021. "On Stablecoin Price Processes and Arbitrage." In *Financial Cryptography.*

Qin, Kaihua, Liyi Zhou, Pablo Gamito, Philipp Jovanovic, and Arthur Gervais. 2021. "An Empirical Study of DeFi Liquidations: Incentives, Risks, and Instabilities." In *Proceedings of the 21st ACM Internet Measurement Conference,* 336–350.

Rivera, Thomas J, Fahad Saleh, and Quentin Vandeweyer. 2023. "Equilibrium in a DeFi Lending Market." *Available at SSRN 4389890.*

Routledge, Bryan, and Ariel Zetlin-Jones. 2021. "Currency stability using blockchain technology." *Journal of Economic Dynamics and Control:* 104155.

Saengchote, Kanis. 2023. "Decentralized Lending and Its Users: Insights from Compound." *Journal of International Financial Markets, Institutions and Money* 87:101807.

Schär, Fabian. 2021. "Decentralized Finance: On Blockchain-and Smart Contract-Based Financial Markets." *FRB of St. Louis Review.*

Sun, Xiaotong, Charalampos Stasinakis, and Georgios Sermpinis. 2024. "Decentralization illusion in Decentralized Finance: Evidence from tokenized voting in MakerDAO polls." *Journal of Financial Stability* 73:101286.

Zhao, Xi, Peilin Ai, Fujun Lai, Xin Luo, and Jose Benitez. 2022. "Task Management in Decentralized Autonomous organization." *Journal of Operations Management.*

Figures

Figure 1: Distribution of Peg-Price Deviations, Pre- and Post-PSM

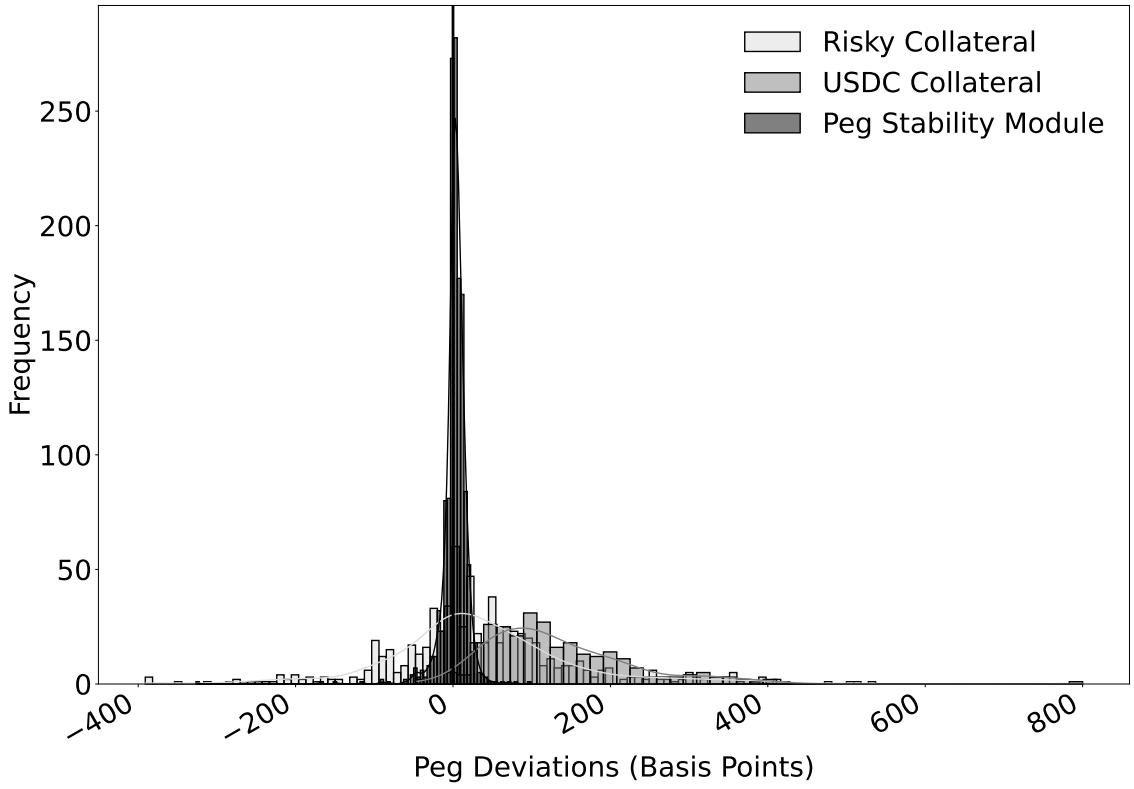

This figure shows the distribution of DAI peg-price deviations (in basis points), calculated as the difference between the DAI/USD price and the 1 USD peg using data from Bitfinex—the earliest exchange with consistent DAI trading. The sample is divided into three regimes: (i) the ETH-only period ("Risky Collateral," light gray); (ii) the transitional phase after USDC was added as collateral ("USDC Collateral," medium gray, March 12 to December 17, 2020); and (iii) the post-PSM regime, following the launch of the Peg Stability Module on December 18, 2020 ("Peg Stability Module," black). Kernel density overlays illustrate the shape of each distribution. The full sample spans April 7, 2018 to September 16, 2024.

Figure 2: Stablecoin Price and Borrowing versus Speculator's Expected Return of Risky Asset E

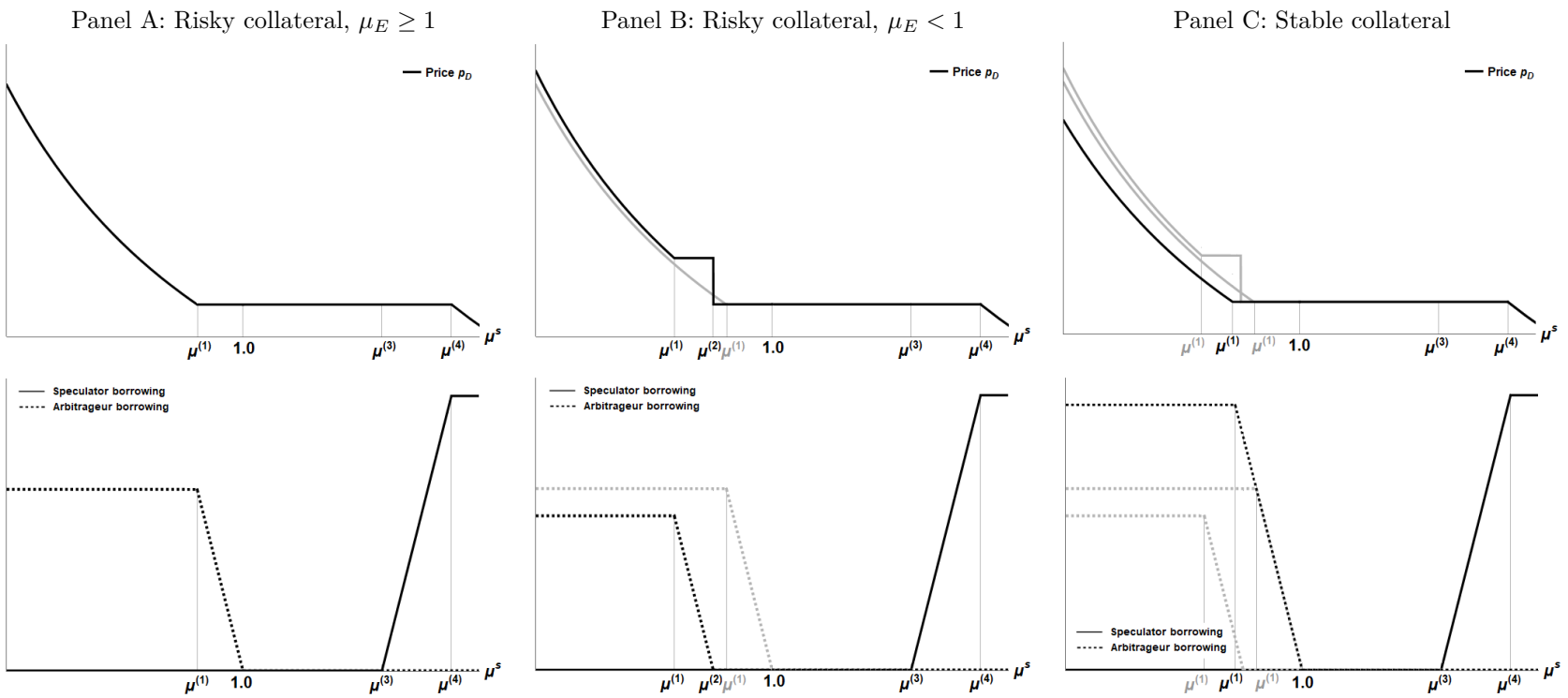

This figure plots price of the stablecoin p_D as a function of the speculator's belief μ^s (top panels) and the amount of stablecoin issued by the speculator and arbitrageur (bottom panels). Panel A corresponds for the risky collateral case with $\mu_E \geq 1$ (we use $\mu_E = 1.08$), Panel B corresponds to the risky collateral case with $\mu_E < 1$ (we use $\mu_E = 0.92$) and Panel C corresponds to the stable collateral case. For Panels A and B we use $\bar{\theta} = 2/3$ and for Panel C we set $\bar{\theta}_U = 1$. The remaining parameters are: $\gamma = 0.2$, $W_0^s = 300$, $W_0^a = 150$, $\sigma_E = 0.07$, $\sigma_U = 0.035$.The gray lines in panels B and C plots the lines from the previous panels for comparison.

Figure 3: Distribution of Leverage for ETH and USDC Vaults

Panel A: Distribution of Average Leverage Ratio par CDP: ETH

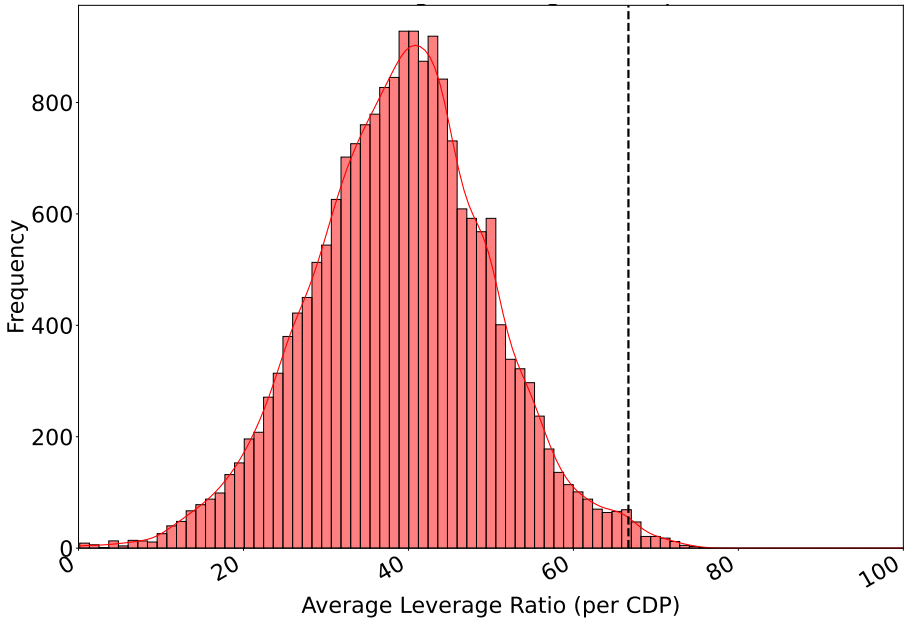

Panel B: Distribution of Average Leverage Ratio par CDP: USDC

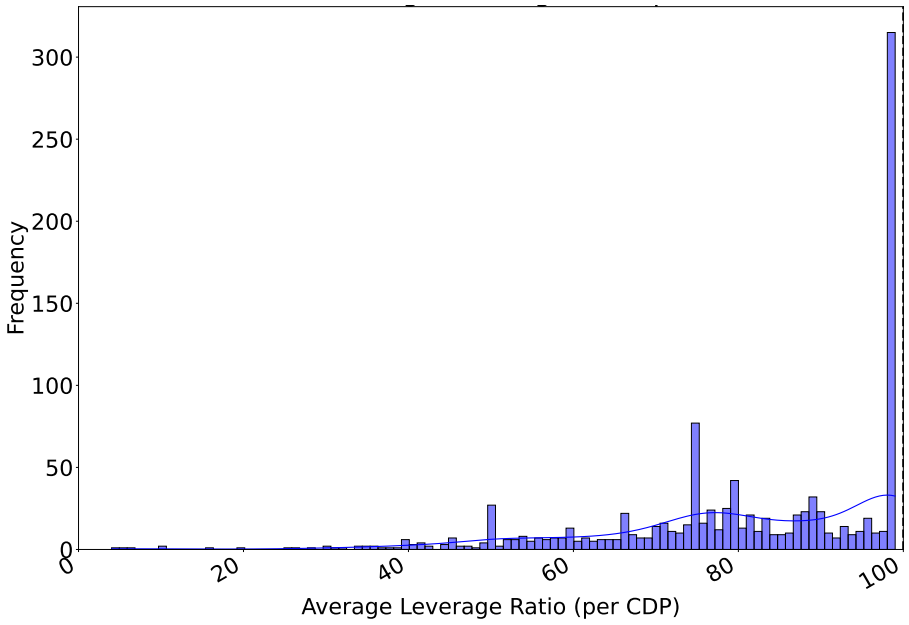

This figure plots the kernel density of the leverage ratio for all CDPs. A CDP is classified as active if it incurred a positive DAI debt balance at any point in its lifetime. The average leverage ratio of all active CDPs is plotted in the histogram. Panel A shows the distribution for ETH CDPs, and Panel B for USDC CDPs. The sample period is from 18 November 2019 to 16 September 2024.

Figure 4: DAI Price, Interest Rates, Supply and Liquidations

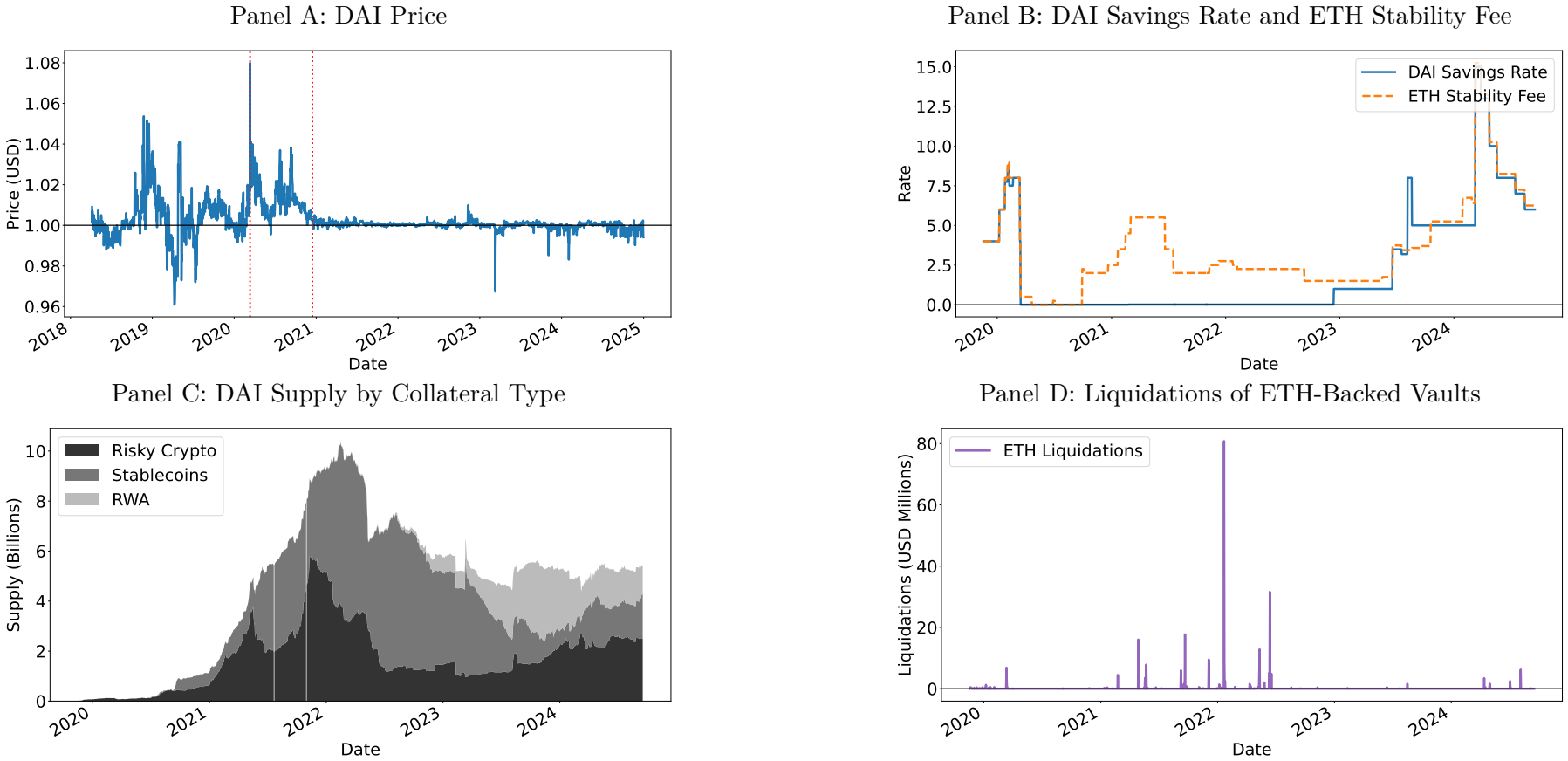

This figure presents four key indicators from the MakerDAO system. Panel A shows the DAI/USD exchange rate on Bitfinex, the earliest exchange with consistent DAI pricing data. Panel B displays the DSR and ETH Stability Fee. Panel C illustrates the supply of DAI broken down by collateral type (risky crypto assets, stablecoins, and real-world assets), measured in billions of USD. Panel D shows total liquidation volumes for ETH-backed CDPs. Red dotted lines indicate the introduction of USDC collateral (March 12, 2020) and the PSM (December 18, 2020). Sample period: April 7, 2018 to September 16, 2024 for panel A, and November 18, 2019 to September 16, 2024 for panels B to D.

Figure 5: Time Series of DAI Borrowings, Collateral and Leverage Ratio for ETH Speculator and Arbitrageur

Panel A: CDP #8463: ETH Speculator

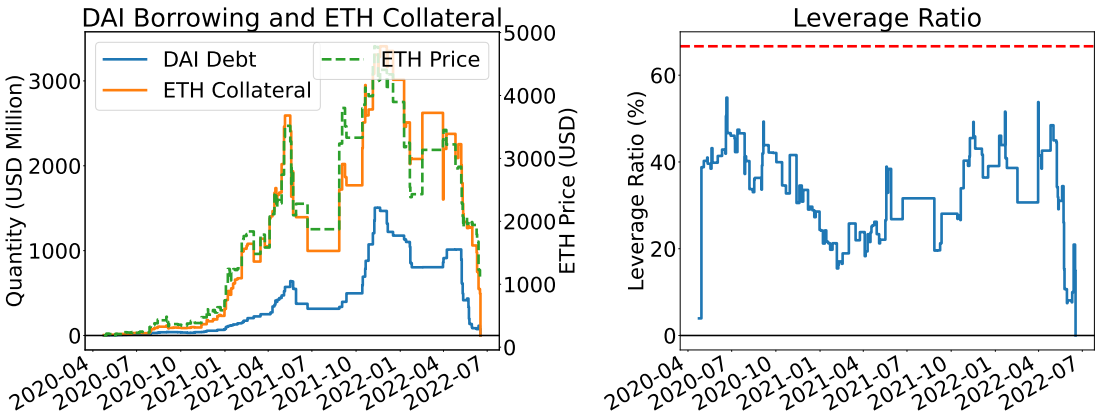

Panel B: CDP #10775: Arbitrageur

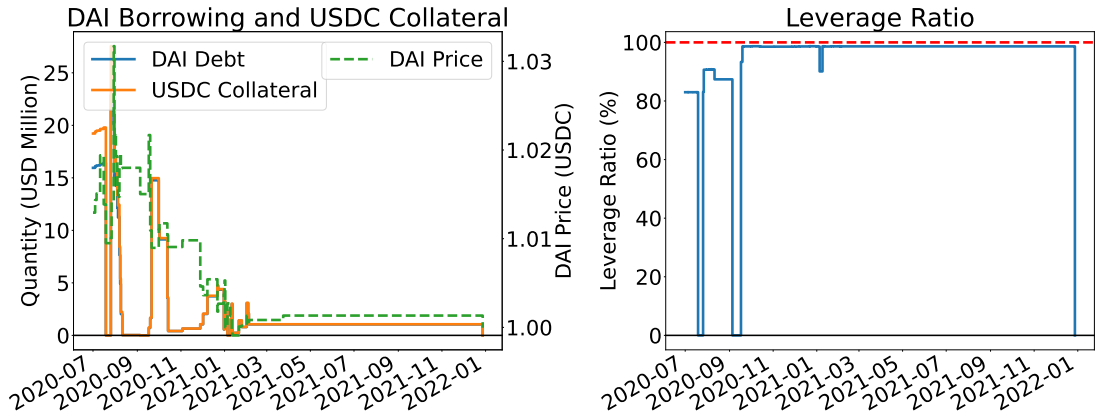

Panel A shows the time series of the leverage ratio (right) and DAI borrowings and ETH collateral (left) for CDP #8463, a representative ETH speculator using DAI to take long leveraged positions in ETH. Panel B presents the same for CDP #10775, a representative arbitrageur who is borrowing DAI to conduct arbitrage activity. The DAI price is quoted in USDC and is based on the DAI/USDC pair trading on Coinbase.

Figure 6: DAI Limits to Arbitrage: Case Studies

Panel A: March 2020 'Black Thursday'

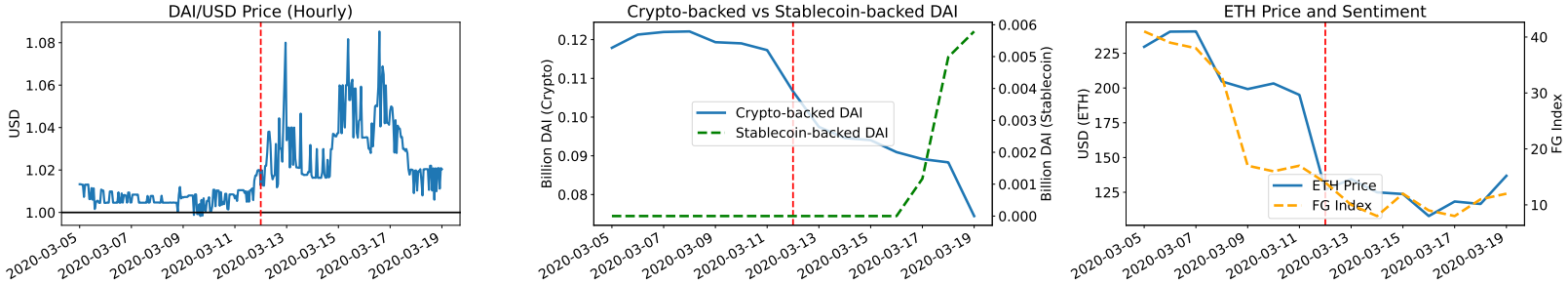

Panel B: May 2021 Flash Crash

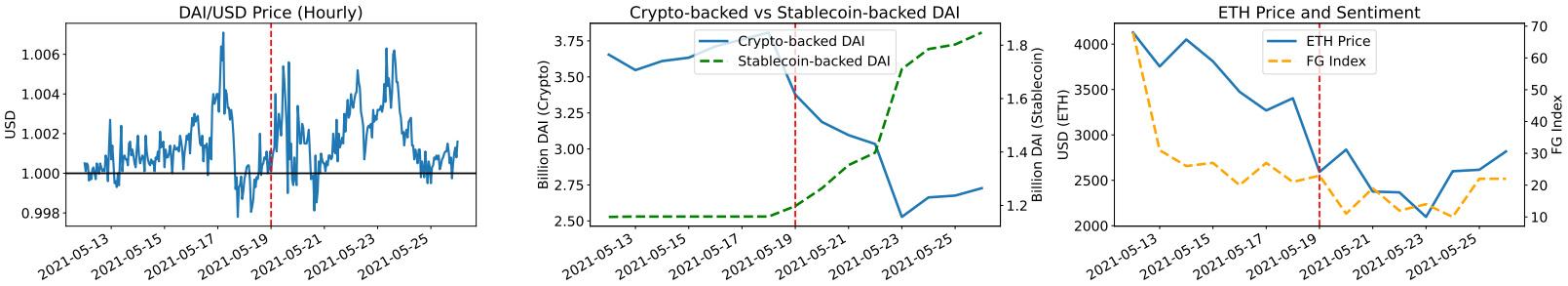

Panel C: March 2023 USDC De-pegging Event

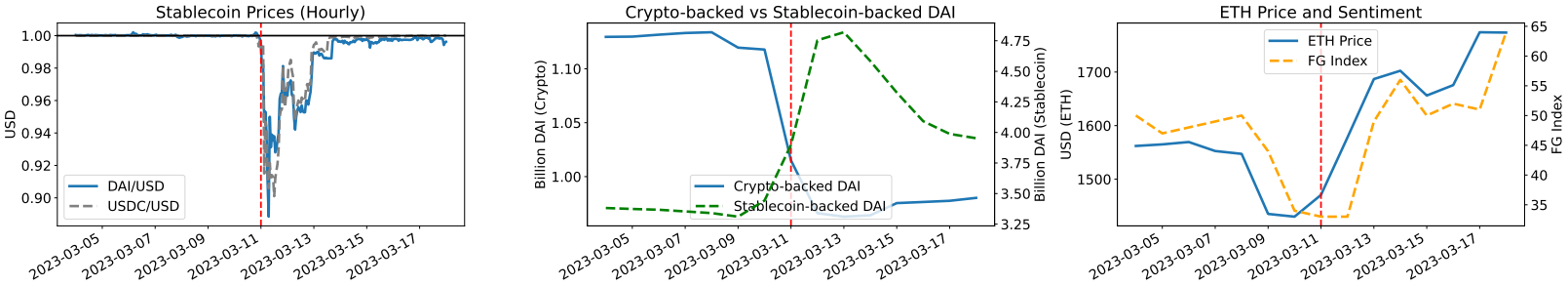

These panels show daily data around major stress episodes in the MakerDAO system. Panel A shows the collapse of ETH and the initial use of USDC as collateral during the March 2020 'Black Thursday' event. Panel B captures the May 2021 flash crash, when ETH prices dropped sharply. Panel C plots dynamics around the March 2023 USDC de-pegging following the collapse of Silicon Valley Bank. Each panel shows the DAI/USD peg, the composition of DAI supply (crypto-backed vs. stablecoin-backed), ETH price and sentiment. Red dashed lines denote the crisis date in each episode.

Figure 7: DAI Limits to Arbitrage

Panel A: Share of Stable Collateral

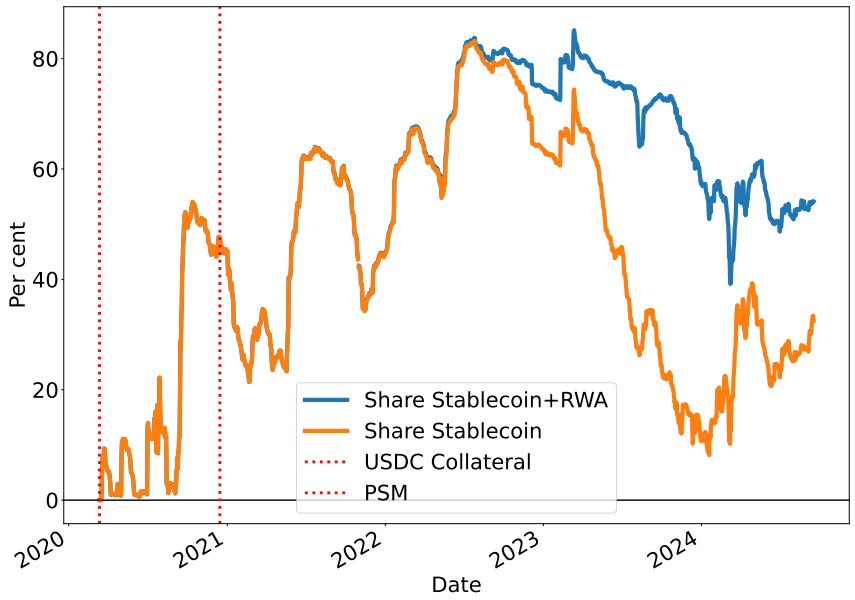

Panel B: Share of DAI Backed by the PSM

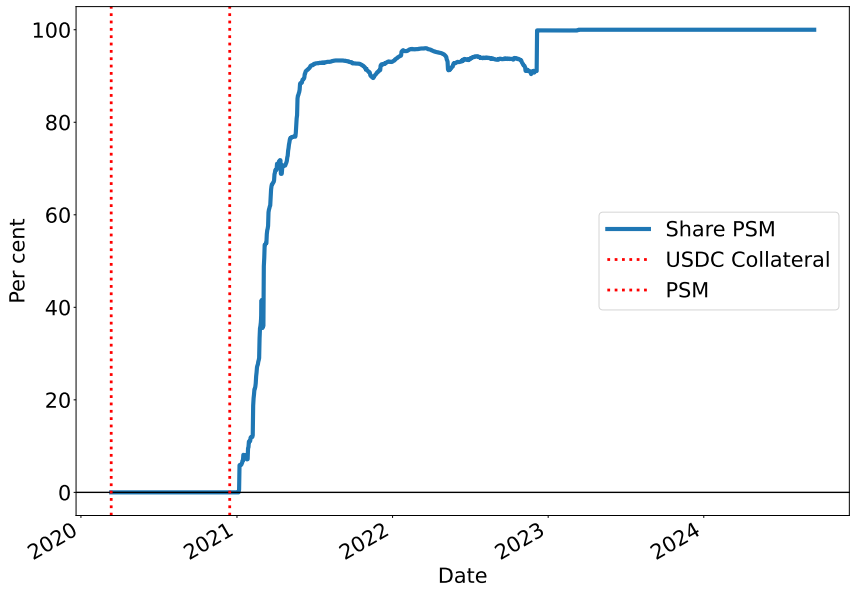

Panel A plots the evolution of the share of DAI backed by safe collateral. It includes a measure inclusive of RWA. The vertical lines indicate the introduction of USDC as collateral in March 2020 and the implementation of the Peg Stability Module (PSM) in December 2020. Panel B plots the share of total DAI supply that is backed by assets held via the PSM. A value closer to 1 indicates a greater proportion of DAI minted against PSM-held stablecoins rather than against riskier collateral types. Both panels are based on daily data.

Figure 8: Impulse Responses of DAI Price to ETH Return (Perpetual Futures Proxy), Policy Parameters, Liquidations, Supply and Demand Proxies

Panel A: ETH Return (Perpetual Futures Proxy)

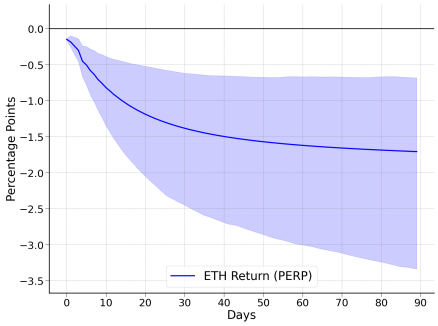

Panel B: Stability Fee (ETH)

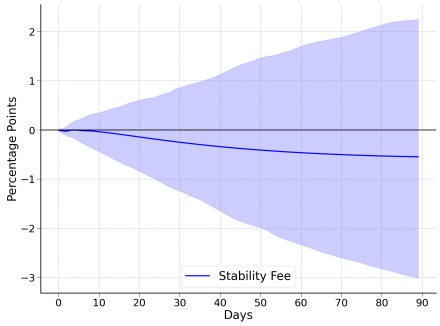

Panel C: DAI Savings Rate (DSR)

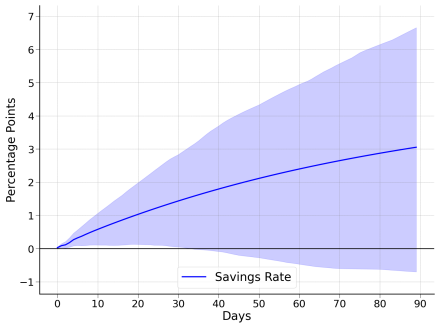

Panel D: Liquidations (ETH)

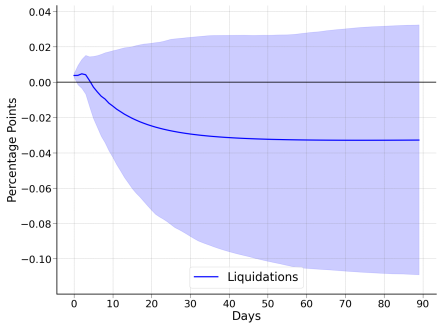

Panel E: DAI Supply

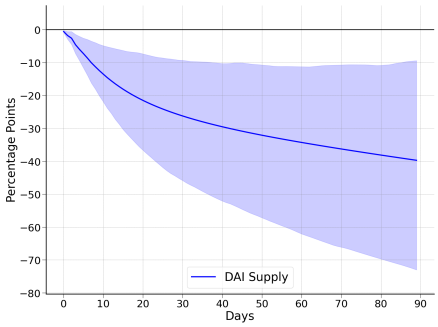

Panel F: DAI Demand Proxy

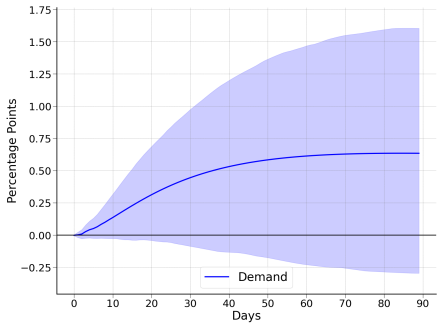

This figure presents the cumulative impulse response functions (IRFs) of the DAI price to shocks in ETH market variables and monetary fundamentals. Panel A shows the effect of an expected ETH return shock (perpetual proxy), Panel B the ETH stability fee, and Panel C the DSR. Panels D through F show the effects of ETH-collateral liquidations, log DAI supply, and a DAI demand proxy, respectively. The IRFs are estimated from a structural VAR with 1,000 wild bootstrap replications. Solid lines indicate the mean response, and shaded areas represent 95% confidence bands. The sample spans from 18 November 2019 to 16 September 2024.

Tables

Table 1: CDP: Breakdown by Asset Type

Asset	Active CDPs	Liquidated	Share Liquidated (%)
ETH	19562	1261	6.45
WBTC	3116	287	9.21
USDC	1090	562	51.56
wstETH	1062	320	30.13
BAT	672	220	32.74
LINK	508	247	48.62
YFI	303	117	38.61
UNI	273	132	48.35
GUNIV3DAIUSDC2	248	0	0.00
GUNIV3DAIUSDC1	227	0	0.00
RENBTC	148	91	61.49
AAVE	122	57	46.72
KNCL	115	32	27.83
UNIV2USDCETH	98	50	51.02
UNIV2DAIETH	98	33	33.67
rETH	93	71	76.34
LRC	90	29	32.22
ZRX	88	31	35.23
UNIV2DAIUSDC	68	0	0.00
TUSD	58	44	75.86
MANA	56	9	16.07
COMP	50	22	44.00
UNIV2UNIETH	39	4	10.26
steCRV	39	22	56.41
UNIV2WBTCETH	36	19	52.78
BAL	34	18	52.94
MATIC	30	23	76.67
USDT	26	9	34.62
USDP	24	18	75.00
UNIV2ETHUSDT	22	2	9.09
GUSD	21	17	80.95
UNIV2LINKETH	18	8	44.44
UNIV2WBTCDAI	14	11	78.57
UNIV2AAVEETH	4	2	50.00
GNO	1	0	0.00

This table presents a breakdown of active CDPs by collateral asset type. A CDP is classified as active if it incurred a positive DAI debt balance at any point in its lifetime. The table reports the total number of such CDPs by asset, the number that experienced at least one liquidation event, and the corresponding percentage of CDPs that were liquidated. The sample covers the period from 18 November 2019 to 16 September 2024.

Table 2: Summary Statistics: CDP Data

Variable	Count	Mean	Std	Min	25%	50%	75%	Max
Panel A: ETH-backed CDPs								
Average Leverage	19562	0.39	0.11	0.00	0.32	0.39	0.46	1.17
Max Debt (DAI Million)	19562	0.51	11.65	0.00	0.00	0.01	0.07	1506.23
Max Collateral (ETH Million)	19562	0.00	0.01	0.00	0.00	0.00	0.00	0.88
Liquidations	19562	0.07	0.25	0.00	0.00	0.00	0.00	3.00
Panel B: USDC-backed CDPs								
Average Leverage	1090	0.81	0.18	0.04	0.72	0.83	0.99	0.99
Max Debt (DAI Million)	1090	0.95	4.14	0.00	0.00	0.04	0.47	72.87
Max Collateral (USDC Million)	1090	0.99	4.27	0.00	0.00	0.06	0.50	75.00
Liquidations	1090	0.70	1.02	0.00	0.00	1.00	1.00	11.00

This table presents summary statistics of key variables for individual active CDPs. Active CDPs are defined as CDPs are borrowers that have a positive amount of DAI debt at some point during the lifetime of the CDP (i.e. DAI borrowing greater than zero). *DAI Debt* and *Collateral* are measured in USD. *Average Leverage* is the average daily ratio of DAI debt to collateral value. Max Debt and Collateral are the maximum amount of DAI borrowing and collateral deposited for each CDP. *Liquidations* counts the number of liquidation events per CDP. Panel A is for CDPs backed by ETH collateral, and panel B is for CDPs backed by USDC collateral. The sample spans from November 18, 2019 to September 16, 2024.

Table 3: Summary Statistics: System Parameters and Aggregate Data

Variable	Count	Mean	Std	Min	25%	50%	75%	Max
Panel A: DAI Supply and Liquidations (Millions USD)								
Total DAI Supply (TotalDAI_t)	1763	4583.64	2827.02	1.69	1656.04	5237.03	6064.32	10374.52
Stablecoin-backed DAI ($\text{SC}_{\text{DAI},t}$)	1763	2262.44	1963.98	0.00	511.14	1582.84	3748.11	6645.05
RWA-backed DAI ($\text{RWA}_{\text{DAI},t}$)	1763	583.03	837.76	0.00	0.00	33.96	1098.33	2890.43
Crypto-backed DAI ($\text{Crypto}_{\text{DAI},t}$)	1763	1738.18	1259.82	1.69	1005.53	1511.65	2425.48	5819.06
Total Liquidations (Debt)	1765	1165.43	7824.86	0.00	0.00	8.27	168.09	231202.64
ETH Liquidations (Debt)	1765	156.09	2227.68	0.00	0.00	0.00	0.00	80812.99
Panel B: DAI Price and System Parameters								
DAI/USD Price ($s_t^{\text{DAI/USD}}$)	1765	1.00	0.01	0.97	1.00	1.00	1.00	1.08
DAI/USDC Price ($s_t^{\text{DAI/USDC}}$)	968	1.00	0.01	0.99	1.00	1.00	1.00	1.06
DAI Savings Rate (DSR)	1763	2.23	3.37	0.00	0.01	0.01	5.00	15.00
Stability Fee (ETH)	1762	3.54	2.90	0.00	1.50	2.25	5.25	15.25
DAI Price Volatility (σ_t^{DAI})	1765	49.97	55.00	0.00	15.49	30.85	64.11	572.88
DAI/USD Deviation Pre-PSM ($p_t^{\text{DAI/USD}} - 1$)	396	102.05	98.69	-84.80	34.75	86.50	149.75	800.00
DAI/USD Deviation Post-PSM ($p_t^{\text{DAI/USD}} - 1$)	1369	2.38	17.81	-326.60	-1.10	3.00	10.00	99.00
DAI/USDC Deviation Pre-PSM ($p_t^{\text{DAI/USDC}} - 1$)	396	83.43	93.76	-64.13	15.87	67.26	126.60	567.72
DAI/USDC Deviation Post-PSM ($p_t^{\text{DAI/USDC}} - 1$)	572	4.67	7.89	-10.00	-0.96	2.11	9.47	52.88
Share of Risky Collateral (ShareRisky_t)	1763	0.49	0.26	0.15	0.27	0.43	0.64	1.00
Panel C: Risky Cryptocurrency Returns								
ETH Price (p_t^{ETH})	1765	1873.86	1163.95	110.30	1149.98	1816.05	2745.51	4811.90
ETH Return (R_t^{ETH})	1765	0.24	4.46	-43.32	-1.80	0.13	2.26	26.46
Sentiment-based Return Proxy ($\tilde{R}_t^{\text{Sent}}$)	1765	48.49	22.47	6.00	28.00	49.00	70.00	95.00
ETH Volatility (σ_t^{ETH})	1765	358.66	245.00	0.00	208.94	306.80	447.66	3209.59

This table reports summary statistics for key variables used in the empirical analysis. **Panel A** reports data on DAI issuance, broken down by collateral type: stablecoins, real-world assets (RWA), and crypto assets. It also includes daily liquidation volumes in USD. **Panel B** presents statistics for the DAI/USD and DAI/USDC exchange rates, deviations from peg before and after the introduction of the PSM (in basis points), as well as the DSR, ETH Stability Fee, and DAI price volatility. **Panel C** summarizes ETH market data: price levels, returns, a sentiment-based return proxy, and annualized volatility. Return variables are expressed in percent. The sample spans daily data from November 18, 2019 to September 16, 2024, except for the DAI/USD price ($s_t^{\text{DAI/USD}}$), which is available from April 7, 2018.

Table 4: Determinants of CDP DAI Borrowing - ETH Collateral

	(1)	(2)	(3)	(4)
	$DAI_{i,t}$			
$\mathbb{E}_t[\tilde{R}^{ETH}_{perp}]$	0.0500***		0.0542***	
	(0.00891)		(0.0126)	
$\mathbb{E}_t[\tilde{R}^{ETH}_{sent}]$		0.0969**		0.102**
		(0.0402)		(0.0412)
$\tilde{R}^{ETH}_t$			-0.00482	0.0480***
			(0.0128)	(0.0104)
$p^{DAI}_t - 1$	0.0388***	0.0302*	0.0371***	0.0780***
	(0.0111)	(0.0175)	(0.0121)	(0.0260)
Constant	0.0217**	0.0254**	0.0227***	-0.0225
	(0.00880)	(0.0103)	(0.00759)	(0.0176)
Controls	✓	✓	✓	✓
IV	✓	✓	✓	✓
Observations	180,280	181,690	180,280	181,690
Number of CDP IDs	19,319	19,460	19,319	19,460

Robust standard errors in parentheses
*** p<0.01, ** p<0.05, * p<0.1

This table presents panel IV regression estimates of individual CDP DAI borrowing, $DAI_{i,t}$, defined as the change in outstanding debt (in millions of DAI), regressed on ETH return proxies and DAI peg deviations:

$$Y_{i,t} = \alpha_i + \beta_1 \mathbb{E}_t[\tilde{R}^{ETH}] + \beta_2 (p^{DAI}_t - 1) + \text{Controls}_t + u_{i,t},$$

where $\mathbb{E}_t[\tilde{R}^{ETH}]$ represents either expected ETH return from perpetual futures ($\mathbb{E}_t[\tilde{R}^{ETH}_{perp}]$), the sentiment-based proxy $\mathbb{E}_t[\tilde{R}^{ETH}_{sent}]$, or a combination of those with the actual return $\tilde{R}^{ETH}_t$. All return measures are standardized. The variable $p^{DAI}_t - 1$ denotes the deviation of the secondary market DAI/USD price from parity.Controls include lagged DAI borrowing and savings rates and ETH intraday volatility. The peg-price deviation is instrumented using its lag, ETH return and volatility, and lagged DAI borrowing and savings rates. Regressions include CDP fixed effects with standard errors clustered at the CDP level. Sample: Nov 18, 2019 – Sep 16, 2024.

Table 5: Determinants of CDP DAI Borrowing - USDC Collateral

	(1)	(2)	(3)	(4)
	$DAI_{i,t}$			
$\mathbb{E}_t[\tilde{R}^{ETH}_{perp}]$	0.145		0.364	
	(0.183)		(0.247)	
$\mathbb{E}_t[\tilde{R}^{ETH}_{sent}]$		-0.276**		-0.281**
		(0.140)		(0.139)
$\tilde{R}^{ETH}_t$			-0.253	0.0703
			(0.189)	(0.167)
$p_t^{DAI/USDC} - 1$	0.109	0.107	0.139	0.0791
	(0.167)	(0.170)	(0.170)	(0.176)
Constant	-0.122	0.165	-0.165	0.164
	(0.418)	(0.458)	(0.418)	(0.458)
Controls	✓	✓	✓	✓
IV	✓	✓	✓	✓
Observations	3,051	3,051	3,051	3,051
Number of CDP IDs	1,077	1,077	1,077	1,077

Robust standard errors in parentheses
*** p<0.01, ** p<0.05, * p<0.1

This table presents panel IV regression estimates of individual CDP DAI borrowing, $DAI_{i,t}$, defined as the change in outstanding debt (in millions of DAI), regressed on ETH return proxies and DAI peg deviations:

$$Y_{i,t} = \alpha_i + \beta_1 \mathbb{E}_t[\tilde{R}^{ETH}] + \beta_2 (p_t^{DAI/USDC} - 1) + \text{Controls}_t + u_{i,t},$$

where $\mathbb{E}_t[\tilde{R}^{ETH}]$ denotes either expected ETH return from perpetual futures ($\mathbb{E}_t[\tilde{R}^{ETH}_{perp}]$), the sentiment-based proxy $\mathbb{E}_t[\tilde{R}^{ETH}_{sent}]$, or a combination of those with the actual return $\tilde{R}^{ETH}_t$. All return variables are standardized. The variable $p_t^{DAI/USDC} - 1$ denotes the deviation of the secondary market DAI/USDC price from parity. Controls include lagged DAI borrowing and savings rates, ETH intraday volatility. The peg-price deviation is instrumented using its lag, ETH return and volatility, USDC volatility, and lagged DAI borrowing and savings rates. Regressions include CDP fixed effects with standard errors clustered at the CDP level. The sample period is from November 18, 2019 to September 16, 2024.

Table 6: DAI Peg-Price Fundamentals

	(1)	(2)	(3)	(4)
	$p_t^{DAI} - 1$			
$\mathbb{E}_t[\tilde{R}^{\text{ETH}}_{\text{perp}}]$	-0.178**			
	(0.078)			
$\mathbb{E}_t[\tilde{R}^{\text{ETH}}_{\text{perp}}] \times$ Share Safe$_t$	0.381**			
	(0.172)			
$\mathbb{E}_t[\tilde{R}^{\text{ETH}}_{\text{Sent}}]$		-0.072**		
		(0.029)		
$\mathbb{E}_t[\tilde{R}^{\text{ETH}}_{\text{Sent}}] \times$ Share Safe$_t$		0.166**		
		(0.071)		
$\mathbf{1}^{(\text{Extreme Neg})}_{\text{perp}}$			0.549	
			(0.405)	
$\mathbf{1}^{(\text{Extreme Neg})}_{\text{perp}} \times$ Share Safe$_t$			-2.100	
			(1.428)	
$\mathbf{1}^{(\text{Extreme Neg})}_{\text{sent}}$				0.446*
				(0.250)
$\mathbf{1}^{(\text{Extreme Neg})}_{\text{sent}} \times$ Share Safe$_t$				-0.841*
				(0.488)
Share Safe$_t$	-0.162***	-0.136***	-0.129***	-0.145***
	(0.041)	(0.046)	(0.038)	(0.047)
$p_{t-1}^{DAI} - 1$	0.849***	0.828***	0.834***	0.809***
	(0.049)	(0.053)	(0.054)	(0.052)
Constant	0.127**	0.149*	0.120	0.164*
	(0.064)	(0.088)	(0.085)	(0.087)
Controls	✓	✓	✓	✓
IV	✓	✓	✓	✓
R^2	0.690	0.461	0.488	0.413
Observations	1,754	1,762	1,762	1,762

Robust standard errors in parentheses
**** p<0.01, ** p<0.05, * p<0.1*

This table presents IV estimates of DAI peg-price deviations (in percentage points) regressed on ETH return proxies, the share of safe collateral backing DAI, and their interactions. Columns (1) and (3) use expected ETH returns from perpetual futures; Columns (2) and (4) use sentiment-based proxies. Columns (3) and (4) additionally include indicators for extreme negative return episodes: returns below -2σ for the perpetual proxy and -1.5σ for the sentiment proxy.
The estimated equation in Columns (1) and (2) is:

$$p_t^{DAI} - 1 = \alpha + \beta_1 \mathbb{E}_t[\tilde{R}^{ETH}] + \beta_2 \mathbb{E}_t[\tilde{R}^{ETH}] \times \text{Share Safe}_t + \beta_3 \text{Controls}_t + u_t$$

ETH liquidations and DAI velocity are treated as endogenous variables and instrumented using their own lags, along with the lagged ETH Stability Fee and DSR. All return variables are standardized. Controls include lagged peg deviations and ETH volatility. Sample period: November 18, 2019 to September 16, 2024.

Table 7: The Effect of Safe Collateral Composition on DAI Peg Stability

	(1) $\lvert p_t^{DAI} - 1 \rvert$	(2) $\lvert p_t^{DAI} - 1 \rvert$	(3) $\lvert p_t^{DAI} - 1 \rvert$
Share Safe	-0.302***		-0.150*
	(0.099)		(0.090)
Share $\text{Safe}_{\text{vault}}$		-0.062	
		(0.068)	
Share Safe_{psm}		-0.312***	
		(0.101)	
Share Safe $\times \mathbf{1}\{p_t^{DAI} > 1\}$			-0.229***
			(0.067)
$\mathbf{1}\{p_t^{DAI} > 1\}$			0.156***
			(0.038)
$\lvert p_{t-1}^{DAI} - 1 \rvert$	0.758***	0.744***	0.741***
	(0.074)	(0.079)	(0.076)
Constant	0.214*	0.208*	0.111
	(0.118)	(0.113)	(0.107)
Controls	✓	✓	✓
R^2	0.735	0.737	0.739
Observations	1,761	1,761	1,761

Robust standard errors in parentheses
*** p<0.01, ** p<0.05, * p<0.1

This table presents OLS regression estimates examining the relationship between DAI peg-price stability and the composition of safe collateral. The dependent variable is the absolute peg deviation $|p_t^{DAI} - 1|$, measured in percentage points. Column (1) includes the aggregate share of safe collateral. Column (2) separates the share into vault-based and PSM-based safe collateral. Column (3) includes an interaction with an indicator for positive peg deviations ($\mathbf{1}\{p_t^{DAI} > 1\}$). The estimated regression is:

$$|p_t^{DAI} - 1| = \alpha + \beta_1 \text{ShareSafe}_t^{(i)} + \beta_2 \text{ShareSafe}_t^{(i)} \times \mathbf{1}\{p_t^{DAI} > 1\} + \text{Controls}_t + \varepsilon_t,$$

where $\text{ShareSafe}_t^{(i)}$ denotes the share (bounded between 0 and 1) of DAI backed by safe collateral, either aggregated, via USDC vaults, or via the PSM. Controls include ETH volatility, DAI Stability Fee, ETH Liquidations, and a proxy fot transactional demand (DAI Velocity). Standard errors are robust to heteroscedasticity. The sample spans November 18, 2019 to September 16, 2024.

Online Appendix to

"Decentralized Stablecoins and Collateral Risk"

(Not for publication)

We provide a roadmap of each section of our appendix:

1. Appendix A provides supplementary figures and explanations of DAI creation and liquidation mechanics within the Maker Protocol.

2. Appendix B provides model derivations and formal proofs for the theoretical framework, including equilibrium conditions and agent optimization.

3. Appendix C provides robustness tests based on CDP-level borrowing regressions:

    - Section A.3.1 explores variation across CDPs by trading frequency (sophistication).
    - Section A.3.2 tests for nonlinearities in ETH return exposure.
    - Section A.3.3 evaluates alternative collateral (WBTC).

4. Appendix D provides supplementary figures reporting impulse responses from a structural VAR framework. These IRFs show the dynamic response of the DAI price to shocks in ETH returns, monetary policy levers (DSR and stability fees), liquidations, and transactional demand proxies.

5. Appendix E presents robustness tests for DAI peg efficiency, including a threshold autoregressive model showing regime shifts in arbitrage response before and after the PSM.

A Definitions: CDP and liquidation process

A.1 DAI Creation

Figure A1: Process of DAI creation

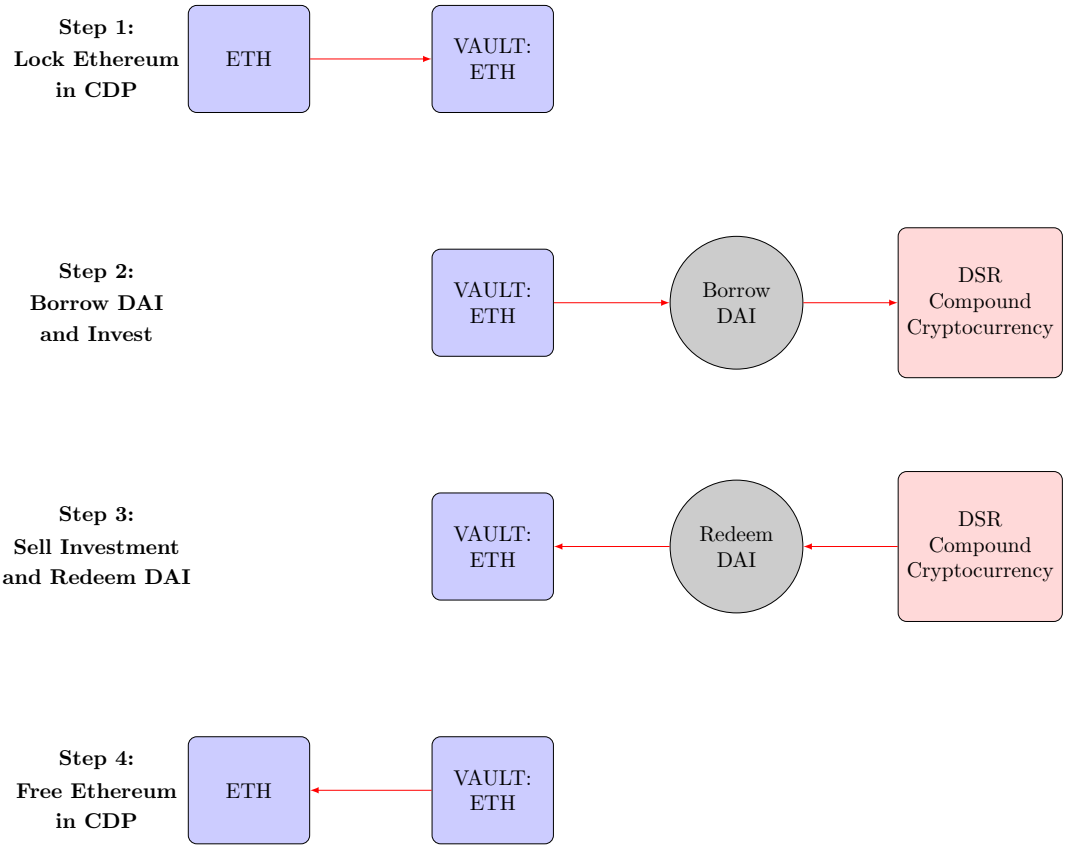

This figure illustrates the steps of depositing dollar wealth into a CDP to create DAI tokens. In borrowing a fraction of ETH collateral as DAI to invest in an alternative currency. At the conclusion of the investment horizon, the investor sells investment for DAI tokens, redeems their DAI tokens and frees their ETH collateral.

A.2 DAI Liquidation Mechanism

Each vault has a maximum leverage ratio, which we denote as Leverage Ratiomax. For ETH collateral, the maximum DAI that can be borrowed is two-thirds of the dollar value of the ETH collateral, hence Leverage ratio$_{max} = \frac{2}{3}$. The Maker Protocol calculates a real-time liquidation price using Equation (25), which is the price of collateral at which the Vault leverage is equal to the maximum leverage ratio. If the collateral price falls below the liquidation price, a liquidation event is triggered.

$$\text{Liquidation price} = \frac{\text{Generated DAI}}{\text{Collateral amount}} \times \frac{1}{\text{Leverage ratio}_{max}} \times 100 \tag{25}$$

In a liquidation event, the investor is required to repay the DAI debt using their remaining collateral and pay a liquidation penalty. For example, at an ETH price of 100 USD, DAI borrowings of 100 USD, and 2 ETH, the leverage ratio is 50%, and the liquidation price is 75 USD, as calculated in Equation (25). Suppose the ETH price falls below the liquidation price to 60 USD in the next period. As the new ETH price is lower than the liquidation price, DAI borrowings are liquidated to zero. To pay off the DAI loan, the investor needs to cover the total value of the loan through their ETH collateral, which is 120 USD at the new price. Subtracting the value of the DAI loan gives a post-liquidation amount of ETH collateral equal to 20 USD or $\frac{1}{3}$ ETH. To pay off the loan, the smart contract forces an auction of $\frac{5}{3}$ ETH.

Figure A2: DAI Liquidation Mechanism

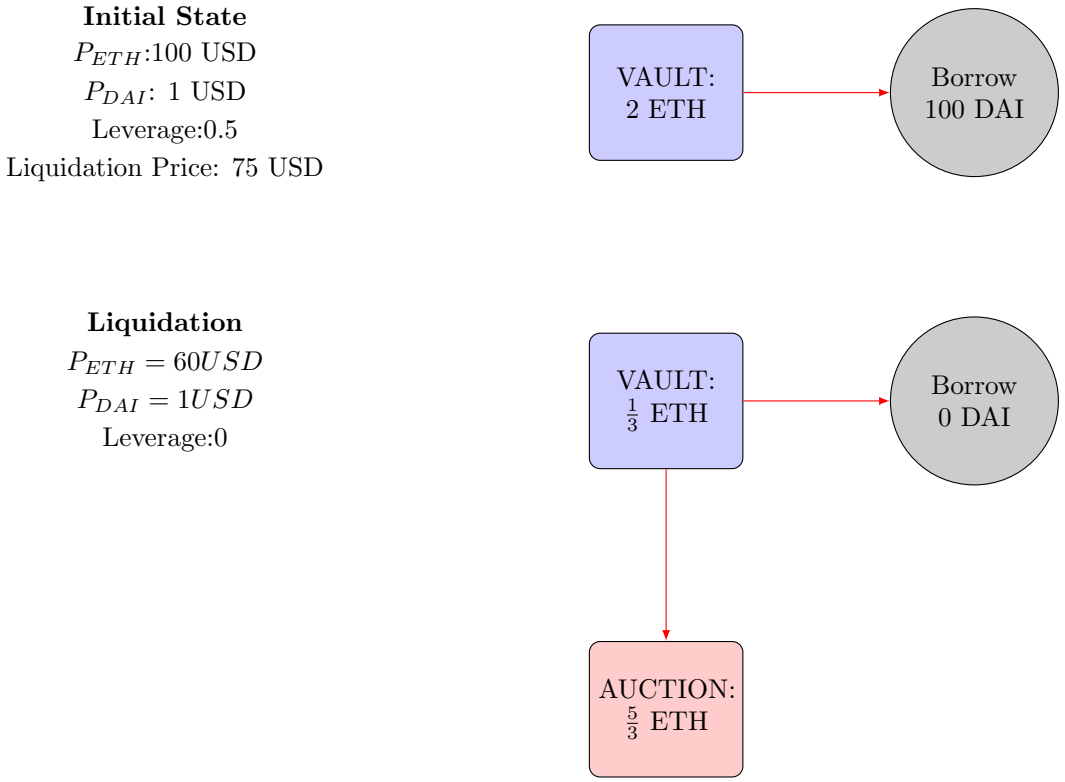

This figure illustrates the steps of liquidation for a hypothetical CDP. In the initial state, the investor deposits 2 ETH in a vault, and borrows 100 DAI tokens. At prices of $P_{ETH} = 100$ USD and $P_{DAI} = 1$ USD, the leverage of the CDP is 0.50. In the liquidation period, the price of ETH declines to 60 USD. This triggers liquidation as the price is less than the liquidation price of 75 USD. DAI borrowings are forced to zero. Keepers auction off 100 USD worth of collateral to pay off the DAI loan, this is equal to $\frac{5}{3}$ ETH at the new price of 60 USD. The new amount of ETH in the vault is $\frac{1}{3}$ ETH. This example is a simplified setting as it ignores additional liquidation costs, such as a liquidation penalty or the potential for fire sale auction prices of ETH.

B Model Proofs

Proof of Proposition 1.

In order to solve for the equilibrium price, we first derive optimal demands of the arbitrageur and the speculator.

Optimal demand of the arbitrageur.

Consider the case when the arbitrageur takes a long position in asset D: $\Delta^a \geq 0$. In this case, $p_D \leq 1$ due to the non-speculation constraint (8). If $p_D = 1$, the arbitrageur is indifferent among any $0 \leq \Delta^a \leq W_0^a$ as any of such value generates zero expected profit and satisfies constraint (8). Hence, the specific value of Δ^a is determined by the market clearing condition. If $p_D < 1$, the expected profit of the arbitrageur is increasing with Δ^a and again, any value $0 \leq \Delta^a \leq W_0^a$ satisfies the constraints.

Consider now the case when the arbitrageur takes a short position in asset D ($\Delta^a < 0$) and issues stablecoins via the protocol. For the non-speculation constraint (8) to hold, the price should satisfy $p_D \geq 1$. In order to satisfy the non-negativity of expected profit condition, we have

$$p_D \geq 1 - \frac{1-\mu_E}{\theta}. \tag{26}$$

Since, the expected utility of the speculator decreases as the price increases (this condition will be verified later), the arbitrageur chooses the smallest possible price to satisfy the equilibrium condition of maximization of speculator's expected utility (competitiveness of the arbitrageur), which is $p_D = 1$ whenever $\mu_E \geq 1$ and she chooses the highest possible leverage ratio $\bar{\theta}(\mu_E - \sigma_E)$ whenever $\mu_E < 1$. Hence, the non-negativity of expected profit condition becomes

$$\begin{cases} p_D \geq 1, & \text{if } \mu_E \geq 1, \\ p_D \geq 1 - \frac{1-\mu_E}{\bar{\theta}(\mu_E - \sigma_E)}, & \text{if } \mu_E < 1. \end{cases}$$

The speculator's optimal demand for a long leveraged position.

The expected utility of the speculator who leverages fraction ω^s of his wealth in asset E is given by

$$E(U(\omega^s)) = W_0^s(\mu^s(1+\omega^s p_D) - \omega^s) - \frac{\gamma (W_0^s)^2 (1+\omega^s p_D)^2 \sigma_E^2}{2},$$

for $0 \leq \omega^s \leq \bar{\theta}(\mu^s - \sigma_E)$. To solve the optimization problem of the speculator, we specify

the following Lagrangian function:

$$L(\omega^s) = E(U(\omega^s)) + \lambda_1\omega^s + \lambda_2(\bar{\theta}(\mu^s - \sigma_E) - \omega^s), \quad \lambda_1, \lambda_2 \geq 0.$$

The first-order and complementary slackness conditions are

$$0 = W_0^s(\mu^s p_D - 1) - \gamma(W_0^s)^2(1 + \omega^s p_D)p_D\sigma_E^2 + \lambda_1 - \lambda_2, \tag{27}$$

$$0 = \lambda_1\omega^s, \tag{28}$$

$$0 = \lambda_2(\bar{\theta}(\mu^s - \sigma_E) - \omega^s). \tag{29}$$

We consider the following cases for variable and Lagrange multipliers values:

1. $\omega^s = 0$.

   Condition $\omega^s = 0$ implies that $\lambda_1 \geq 0$ and $\lambda_2 = 0$. The first-order condition (27) becomes $\lambda_1 = -W_0^s(\mu^s p_D - 1) + \gamma(W_0^s)^2 p_D\sigma_E^2$. Hence, $\lambda_1 \geq 0$ is equivalent to

   $$\mu^s \leq \frac{1}{p_D} + \gamma W_0^s\sigma_E^2 \tag{30}$$

2. $0 < \omega^s < \bar{\theta}(\mu^s - \sigma_E)$.

   In this case $\lambda_1 = \lambda_2 = 0$ and the first-order condition (27) transforms to

   $$\omega^s = \frac{(\mu^s p_D - 1)}{\gamma W_0^s p_D^2\sigma_E^2} - \frac{1}{p_D}. \tag{31}$$

   In order to satisfy the initial restriction $0 < \omega^s < \bar{\theta}(\mu^s - \sigma_E)$, the following inequalities should hold:

   $$\frac{1}{p_D} < \frac{(\mu^s p_D - 1)}{\gamma W_0^s p_D^2\sigma_E^2} < \frac{1}{p_D} + \bar{\theta}(\mu^s - \sigma_E). \tag{32}$$

3. $\omega^s = \bar{\theta}(\mu^s - \sigma_E)$.

   In this case $\lambda_1 = 0$ and the first-order condition (27) implies

   $$\lambda_2 = W_0^s(\mu^s p_D - 1) - \gamma(W_0^s)^2(1 + \bar{\theta}(\mu^s - \sigma_E)p_D)p_D\sigma_E^2.$$

   The inequality $\lambda_2 \geq 0$ is equivalent to

   $$\mu^s \geq \frac{1}{p_D} + \gamma W_0^s(1 + \bar{\theta}(\mu^s - \sigma_E)p_D)\sigma_E^2.$$

Combining the three cases, we get the expression for the optimal demand for the speculator's supply of asset D:

$$\omega^s = \min\left\{0, \max\left\{\frac{(\mu^s p_D - 1)}{\gamma W_0^s p_D^2 \sigma_E^2} - \frac{1}{p_D}, \bar{\theta}(\mu^s - \sigma_E)\right\}\right\}. \tag{33}$$

The speculator's optimal demand for a short position.

The expected utility in this case is given by

$$E(U(\omega^s)) = \frac{(1-\omega^s)W_0^s}{p_D} + \omega^s W_0^s \mu^s - \frac{\gamma (W_0^s \omega^s)^2 \sigma_E^2}{2}.$$

for $-1 \leq \omega^s \leq 0$. To solve the optimization problem of the speculator, we specify the following Lagrangian function:

$$L(\omega^s) = E(U(\omega^s)) + \lambda_1(\omega^s + 1) - \lambda_2 \omega^s, \quad \lambda_1, \lambda_2 \geq 0.$$

The first-order and complementary slackness conditions are

$$0 = -\frac{W_0^s}{p_D} + W_0^s \mu^s - \gamma (W_0^s)^2 \omega^s \sigma_E^2 + \lambda_1 - \lambda_2, \tag{34}$$

$$0 = \lambda_1(1 + \omega^s), \tag{35}$$

$$0 = \lambda_2 \omega^s. \tag{36}$$

We consider the following cases for variable and Lagrange multipliers values:

1. $\omega^s = 0$.

   Condition $\omega^s = 0$ implies that $\lambda_2 \geq 0$ and $\lambda_1 = 0$. The first-order condition (34) becomes $\lambda_2 = -\frac{W_0^s}{p_D} + W_0^s \mu^s$. The inequality $\lambda_2 \geq 0$ is equivalent to

   $$\mu^s \geq \frac{1}{p_D}. \tag{37}$$

2. $-1 < \omega^s < 0$.

   In this case $\lambda_1 = \lambda_2 = 0$ and the first-order condition (34) transforms to

   $$\omega^s = \frac{\mu^s - \frac{1}{p_D}}{\gamma W_0^s \sigma_E^2}. \tag{38}$$

   In order to satisfy the initial restriction $-1 < \omega^s < 0$, the following inequalities

should hold:

$$\frac{1}{p_D} - \gamma W_0^s \sigma_E^2 < \mu^s < \frac{1}{p_D}. \tag{39}$$

3. $\omega^s = -1$.

In this case $\lambda_2 = 0$ and the first-order condition (34) implies

$$\lambda_1 = \frac{W_0^s}{p_D} - W_0^s \mu^s + \gamma (W_0^s)^2 \sigma_E^2.$$

The inequality $\lambda_1 \geq 0$ is equivalent to

$$\mu^s \leq \frac{1}{p_D} - \gamma W_0^s \sigma_E^2.$$

Combining the three cases, we get the expression for the optimal demand for the speculator's supply of asset D:

$$\omega^s = \max\left\{-1, \min\left\{\frac{\frac{1}{p_D} - \mu^s)}{\gamma W_0^s \sigma_E^2}, 0\right\}\right\}. \tag{40}$$

Equilibrium price when $\omega^s \geq 0$.

According to Equation (32), the speculator issues positive amount of asset D (that is, $\omega^s > 0$) whenever $\mu^s > \frac{1}{p_D} + \gamma W_0^s \sigma_E^2$, or, equivalently, $p_D > \frac{1}{\mu^s - \gamma W_0^s \sigma_E^2}$. Since in this case the price $p_D \leq 1$ (see condition (8)), the speculator does not leverage his position in E (i.e., $\omega^s = 0$) for any $\mu^s \leq 1 + \gamma W_0^s \sigma_E^2 \equiv \mu^{(3)}$. Once $\mu^s > \mu^{(3)}$ sells asset D and the arbitrageurs can fully absorb the speculator's supply as long as it is smaller than the arbitrageur's capital W_0^a. That is, $\omega^* W_0^s \leq W_0^a$, where

$$\omega^* = \frac{\mu^s p_D - 1}{\gamma p_D^2 W_0^s \sigma_E^2} - \frac{1}{p_D}. \tag{41}$$

This is equivalent to

$$\frac{\mu^s p_D - 1}{\gamma p_D^2 \sigma_E^2} - \frac{W_0^s}{p_D} \leq W_0^a. \tag{42}$$

Note, that the speculator's maximum level of expected utility

$$E(U(\omega^s))|_{\omega^s = \omega^*} = \frac{W_0^s}{p_D} + \frac{\left(\mu - \frac{1}{p_D}\right)^2}{2\gamma\sigma_E^2}$$

is an increasing function of p_D on the interval $\left[\frac{1}{\mu^s - \gamma W_0^s \sigma_E^2}, 1\right]$, so the equilibrium price

that maximizes speculator's expected utility is the maximum possible price satisfying the arbitrageur's constraints is $p_D = 1$, as long as it satisfies condition (42), that is:

$$\mu^s \leq 1 + \gamma\sigma_E^2(W_0^s + W_0^a) \equiv \mu^{(4)}.$$

If $\mu^{(s)} > \mu^{(4)}$, the price $p_D = 1$ violates (42), and hence the market clearing condition (9) because the arbitrageur's capital is not sufficient to fully absorb the speculator's supply. The arbitrageur has to lower the price to reduce the supply of the speculator, so that the market clearing condition holds:

$$\frac{\mu^s p_D - 1}{\gamma p_D^2 \sigma_E^2} - \frac{W_0^s}{p_D} = W_0^a \tag{43}$$

or,

$$p_D = \frac{\mu^s - \gamma\sigma_E^2 W_0^s - \sqrt{(\mu^s - \gamma\sigma_E^2 W_0^s)^2 - 4\gamma\sigma_E^2 W_0^a}}{2\gamma\sigma_E^2 W_0^a} \tag{44}$$

(here we consider only one of the root of the quadratic equation satisfying $p_D \leq 1$).

Finally, the condition $\omega^s = \bar{\theta}(\mu^s - \sigma_E)$ is not binding due to our Assumption (7).

Equilibrium price when $\omega^s < 0$.

According to Equation (39), the speculator buys asset D (in order to short E, $\omega^s < 0$) whenever $\mu^s < \frac{1}{p_D}$, or, equivalently, $p_D < \frac{1}{\mu^s}$. Since the price $p_D \geq 1$ due to non-speculation condition (8), the speculator does not short sell E (i.e., $\omega^s = 0$) for any $\mu^s \geq 1$.

Consider two sub-cases based on the arbitrageur's expectation of collateral return.

1. $\mu_E \geq 1$.

   In this case, according to (26), the arbitrageur is happy to issue asset D at any price $p_D \geq 1$ and absorb the speculator's demand as long as $-\omega^* W_0^s \leq \bar{\theta} W_0^a(\mu_E - \sigma_E)$, where

   $$\omega^* = \frac{\mu^s - \frac{1}{p_D}}{\gamma W_0^s \sigma_E^2}. \tag{45}$$

   This is equivalent to

   $$\mu^s \geq \frac{1}{p_D} - \gamma\sigma_E^2 \bar{\theta} W_0^a(\mu_E - \sigma_E), \tag{46}$$

   or $p_D \geq \frac{1}{\mu^s + \gamma\sigma_E^2 \bar{\theta} W_0^a(\mu_E - \sigma_E)}$ Note, that the speculator's maximum level of expected

utility

$$E(U(\omega^s))|_{\omega^s=\omega^*} = \frac{W_0^s}{p_D} + \frac{\left(\mu^s - \frac{1}{p_D}\right)^2}{2\gamma\sigma_E^2}$$

is a decreasing function of p_D on the interval $\left[1, \frac{1}{\mu^s - \gamma\sigma_E^2 W_0^a}\right]$ (and, consequently, on the sub-interval $\left[1, \frac{1}{\mu^s + \gamma\sigma_E^2 \bar{\theta} W_0^a(\mu_E - \sigma_E)}\right]$). Hence, the equilibrium price that maximizes speculator's expected utility is $p_D = 1$ (the minimum possible price satisfying the arbitrageur's constraints), as long as it satisfies condition (42):

$$\mu^s \geq 1 - \gamma\sigma_E^2 \bar{\theta} W_0^a(\mu_E - \sigma_E) \equiv \mu^{(1)}.$$

If $\mu^{(s)} < \mu^{(1)}$, price $p_D = 1$ violates condition (46), and hence the market clearing condition (9). As a result, the arbitrageur has to increase the price in order to reduce the demand of the speculator, so that

$$-\omega^* W_0^s = \bar{\theta} W_0^a(\mu_E - \sigma_E) \tag{47}$$

or, equivalently,

$$p_D = \frac{1}{\mu^s + \gamma\sigma_E^2 \bar{\theta} W_0^a(\mu_E - \sigma_E)}. \tag{48}$$

2. $\mu_E < 1$.

In this case, according to (26), the arbitrageur is happy to issue units of asset D at any price at any price $p_D = 1 - \frac{\mu_E - 1}{\bar{\theta}(\mu_E - \sigma_E)}$. At the same time, according to Equation (39), $p_D < \frac{1}{\mu^s}$. This leads to a no-trade condition whenever

$$\mu^s \geq \frac{\bar{\theta}(\mu_E - \sigma_E)}{1 - \bar{\theta}\sigma_E - \mu_E(1 - \bar{\theta})} \equiv \mu^{(2)}.$$

If $\mu^s < \mu^{(2)}$ the arbitrageur absorbs the speculator's demand at any price $p_D \geq 1 - \frac{\mu_E - 1}{\bar{\theta}(\mu_E - \sigma_E)}$ as long as $-\omega^* W_0^s \leq \bar{\theta} W_0^a(\mu_E - \sigma_E)$, where ω^* is given in (45). This is equivalent to

$$\mu^s \geq \frac{1}{p_D} - \gamma\sigma_E^2 \bar{\theta} W_0^a(\mu_E - \sigma_E), \tag{49}$$

or $p_D \geq \frac{1}{\mu^s + \gamma\sigma_E^2 \bar{\theta} W_0^a(\mu_E - \sigma_E)}$. Since the speculator's maximum level of expected utility

$$E(U(\omega^s))|_{\omega^s=\omega^*} = \frac{W_0^s}{p_D} + \frac{\left(\mu^s - \frac{1}{p_D}\right)^2}{2\gamma\sigma_E^2}$$

is a decreasing function of p_D on the interval $\left[1, \frac{1}{\mu^s - \gamma\sigma_E^2 W_0^s}\right]$ (and hence on the sub-interval $\left[1, \frac{1}{\mu^s + \gamma\sigma_E^2 \bar{\theta} W_0^a (\mu_E - \sigma_E)}\right]$), the arbitrageur chooses the lowest possible price satisfying her constraints: $p_D = 1 - \frac{\mu_E - 1}{\bar{\theta}(\mu_E - \sigma_E)}$. Hence, the trading happens at this price as long as

$$\mu^s \geq \frac{\bar{\theta}(\mu_E - \sigma_E)}{\bar{\theta}(\mu_E - \sigma_E) - (\mu_E - 1)} - \gamma\sigma_E^2 \bar{\theta} W_0^a (\mu_E - \sigma_E) \equiv \mu^{(1)}.$$

If $\mu^{(s)} < \mu^{(1)}$, price $p_D = 1 - \frac{\mu_E - 1}{\bar{\theta}(\mu_E - \sigma_E)}$ violates (49), and hence the market clearing condition (9). As a result, the arbitrageur has to increase the price in order to reduce the demand of the speculator, so that

$$-\omega^* W_0^s = \bar{\theta} W_0^a (\mu_E - \sigma_E) \tag{50}$$

or, equivalently,

$$p_D = \frac{1}{\mu^s + \gamma\sigma_E^2 \bar{\theta} W_0^a (\mu_E - \sigma_E)}. \tag{51}$$

Finally, the condition $\omega^s = -1$ is not binding due to our Assumption (7).

Q.E.D.

Proposition 2: Whenever the arbitrageur has a choice between a risky and stable collateral, she always chooses the stable collateral and the equilibrium price and issuance of asset D is given by

$$\begin{cases} p_D = \frac{1}{\mu^s + \gamma\sigma_E^2 \bar{\theta}_U W_0^a (1 - \sigma_U)}, & \Delta^a = \bar{\theta}_U W_0^a (1 - \sigma_U), & \text{if } \mu^s < \mu^{(5)}, \\ p_D = 1, & \Delta^a = \frac{(1 - \mu^s)}{\gamma\sigma_E^2}, & \text{if } \mu^s \in [\mu^{(5)}, 1), \\ p_D = 1, & \Delta^a = 0, & \text{if } \mu^s \in [1, \mu^{(3)}], \\ p_D = 1, & \Delta^a = \frac{\mu^s - 1}{\gamma\sigma_E^2} - W_0^s, & \text{if } \mu^s \in (\mu^{(3)}, \mu^{(4)}], \\ p_D = \frac{\mu^s - \gamma\sigma_E^2 W_0^s - \sqrt{(\mu^s - \gamma\sigma_E^2 W_0^s)^2 - 4\gamma\sigma_E^2 W_0^a}}{2\gamma\sigma_E^2 W_0^a}, & \Delta^a = W_0^a, & \text{if } \mu^s > \mu^{(4)}, \end{cases} \tag{52}$$

where

$$\mu^{(5)} = 1 - \gamma\sigma_E^2 \bar{\theta}_U W_0^a (1 - \sigma_U). \tag{53}$$

Proof of Proposition 2.

Let us first establish the equilibrium price in the case when the arbitrageur can only choose the stable collateral. Note that it makes a difference only when the arbitrageur

borrows asset D since otherwise she does not have to use any collateral.

Whenever the arbitrageur takes a short position in asset D ($\Delta^a < 0$) and borrows D using stable collateral, the non-negativity of expected profit condition is reduced to $p_D \geq 1$. She issues asset D at any price $p_D \geq 1$ and absorb the speculator's demand as long as $-\omega^* W_0^s \leq \bar{\theta}_U W_0^a (1 - \sigma_U)$, where ω^s is given in Equation (45). This is equivalent to

$$\mu^s \geq \frac{1}{p_D} - \gamma \sigma_E^2 \bar{\theta}_U W_0^a (1 - \sigma_U), \tag{54}$$

or $p_D \geq \frac{1}{\mu^s + \gamma \sigma_E^2 \bar{\theta}_U W_0^a (1 - \sigma_U)}$. Given that the maximum of speculator's of expected utility is a decreasing function of p_D on the interval $\left[1, \frac{1}{\mu^s + \gamma \sigma_E^2 \bar{\theta}_U W_0^a (1 - \sigma_U)}\right]$ (see the proof of Proposition 1 for details), the equilibrium price that maximizes speculator's expected utility is $p_D = 1$ (the minimum possible price satisfying the arbitrageur's constraints), as long as it satisfies condition (42):

$$\mu^s \geq 1 - \gamma \sigma_E^2 \bar{\theta}_U W_0^a (1 - \sigma_U).$$

If $\mu^{(s)} < 1 - \gamma \sigma_E^2 \bar{\theta}_U W_0^a (1 - \sigma_U)$, then price $p_D = 1$ violates (46), and hence the market clearing condition (9). As a result, the arbitrageur has to increase the price in order to reduce the demand of the speculator, so that

$$-\omega^* W_0^s = \bar{\theta}_U W_0^a (1 - \sigma_U) \tag{55}$$

or, equivalently,

$$p_D = \frac{1}{\mu^s + \gamma \sigma_E^2 \bar{\theta}_U W_0^a (1 - \sigma_U)}. \tag{56}$$

This proves that the equilibrium price if the arbitrageur has only access to stable collateral is given by Equation (52).

Now, suppose the arbitrageur has a choice between stable and risky collateral. Note now that the price of asset D in the case when the arbitrageur uses stable collateral is always smaller or equal than the price of asset D when the arbitrageur uses risky collateral. Since $\frac{\bar{\theta}_U}{\bar{\theta}} > \frac{\mu^E - \sigma_E}{1 - \sigma_U}$ (condition 18), we have $\mu^s + \gamma \sigma_E^2 \bar{\theta}_U W_0^a (1 - \sigma_U) > \mu^s + \gamma \sigma_E^2 \bar{\theta} W_0^a (\mu^E - \sigma_E)$ and the following relationships hold.

Case $\mu_E \geq 1$.

- If $\mu^s \in [1 - \gamma \sigma_E^2 \bar{\theta} W_0^a (\mu_E - \sigma_E), 1]$ we have $p_D^{stable} = p_D^{risky} = 1$;

- If $\mu^s \in [1-\gamma\sigma_E^2\bar{\theta}_U W_0^a(1-\sigma_U), 1-\gamma\sigma_E^2\bar{\theta}W_0^s(\mu_E-\sigma_E)]$ we have $p_D^{stable} = 1 < \frac{1}{\mu^s+\gamma\sigma_E^2\bar{\theta}W_0^a(\mu_E-\sigma_E)} = p_D^{risky}$;
- If $\mu^s < 1-\gamma\sigma_E^2\bar{\theta}_U W_0^a(1-\sigma_U)$ we have $p_D^{stable} = \frac{1}{\mu^s+\gamma\sigma_E^2\bar{\theta}_U W_0^a(1-\sigma_E)} < \frac{1}{\mu^s+\gamma\sigma_E^2\bar{\theta}W_0^a(\mu_E-\sigma_E)} = p_D^{risky}$.

Case $\mu_E < 1$.

- If $\mu^s \in \left[\frac{\bar{\theta}(\mu_E-\sigma_E)}{\bar{\theta}(\mu_E-\sigma_E)-(\mu_E-1)} - \gamma\sigma^2\bar{\theta}W_0^a(\mu_E-\sigma_E), 1\right]$ we have $p_D^{stable} \leq \frac{1}{\mu^s+\gamma\sigma_E^2\bar{\theta}_U W_0^a(1-\sigma_E)} < \frac{1}{\mu^s+\gamma\sigma_E^2\bar{\theta}W_0^a(\mu_E-\sigma_E)} \leq p_D^{risky}$;
- If $\mu^s < \frac{\bar{\theta}(\mu_E-\sigma_E)}{\bar{\theta}(\mu_E-\sigma_E)-(\mu_E-1)} - \gamma\sigma^2\bar{\theta}W_0^a(\mu_E-\sigma_E)$ we have $p_D^{stable} = \frac{1}{\mu^s+\gamma\sigma_E^2\bar{\theta}_U W_0^a(1-\sigma_E)} < \frac{1}{\mu^s+\gamma\sigma_E^2\bar{\theta}W_0^a(\mu_E-\sigma_E)} = p_D^{risky}$.

Since the speculator's expected utility evaluated at point ω^* is a decreasing function of p_D on $[1, \frac{1}{\mu^s+\gamma\sigma_E^2\bar{\theta}_u W_0^a(1-\sigma_U)}]$, the equilibrium price is the smaller among the two prices, which is p_D^{stable}.

Q.E.D.

C CDP Robustness Tests

C.1 Sophisticated Traders

Table A1: Determinants of CDP DAI Borrowing – ETH Collateral, Variation by Transaction Frequency

	(1)	(2)	(3)	(4)
	$DAI_{i,t}$			
	CDP Transaction Count ≥ Median		*CDP Transaction Count < Median*	
$\mathbb{E}_t[\tilde{R}^{ETH}_{perp}]$	0.0728***		0.0201***	
	(0.0143)		(0.00499)	
$\mathbb{E}_t[\tilde{R}^{ETH}_{sent}]$		0.129**		0.0468***
		(0.0632)		(0.0158)
$p_t^{DAI} - 1$	0.0417***	0.0606*	0.0269**	0.0153
	(0.0151)	(0.0328)	(0.0110)	(0.0129)
Constant	0.0357**	0.0270*	0.0227**	0.0271**
	(0.0161)	(0.0143)	(0.00996)	(0.0114)
Controls	✓	✓	✓	✓
IV	✓	✓	✓	✓
Observations	91,917	92,263	88,363	89,427
Number of CDP IDs	1,776	1,776	17,543	17,684

Robust standard errors in parentheses
*** p<0.01, ** p<0.05, * p<0.1

This table presents panel IV regression estimates of individual CDP DAI borrowing, $DAI_{i,t}$, defined as the change in outstanding debt (in millions of DAI), split by CDP activity. Columns (1) and (2) show results for CDPs with DAI borrowing transaction counts above or equal to the median; Columns (3) and (4) include those below the median.

$$Y_{i,t} = \alpha_i + \beta_1 \mathbb{E}_t[\tilde{R}^{ETH}] + \beta_2 (p_t^{DAI} - 1) + \text{Controls}_t + u_{i,t},$$

where $\mathbb{E}_t[\tilde{R}^{ETH}]$ represents either the perpetual futures-based proxy $\mathbb{E}_t[\tilde{R}^{ETH}_{perp}]$ or the sentiment-based proxy $\mathbb{E}_t[\tilde{R}^{ETH}_{sent}]$. All return measures are standardized. $p_t^{DAI} - 1$ is the deviation of the DAI/USD exchange rate from parity. Controls include lagged DAI borrowing and savings rates, ETH intraday volatility. The peg-price deviation is instrumented using its lag, ETH return and volatility, and lagged DAI borrowing and savings rates. Regressions include CDP fixed effects with standard errors clustered at the CDP level. Sample: Nov 18, 2019 – Sep 16, 2024.

C.2 Non-Linearity

Table A2: Determinants of CDP DAI Borrowing – ETH Collateral, Extreme Negative Return Robustness

	(1)	(2)
	$DAI_{i,t}$	
$\mathbb{E}_t[\tilde{R}^{ETH}_{\text{perp}}]$	0.0666***	
	(0.0180)	
$\mathbf{1}^{(\text{Extreme Neg})}_{\text{perp}}$	-0.123	
	(0.121)	
$\mathbb{E}_t[\tilde{R}^{ETH}_{\text{perp}}] \times \mathbf{1}^{(\text{Extreme Neg})}_{\text{perp}}$	-0.0890***	
	(0.0290)	
$\mathbb{E}_t[\tilde{R}^{ETH}_{\text{sent}}]$		0.101**
		(0.0402)
$\mathbf{1}^{(\text{Extreme Neg})}_{\text{sent}}$		2.539*
		(1.489)
$\mathbb{E}_t[\tilde{R}^{ETH}_{\text{sent}}] \times \mathbf{1}^{(\text{Extreme Neg})}_{\text{sent}}$		1.562
		(0.962)
$p_t^{DAI} - 1$	0.0420***	0.0314*
	(0.0142)	(0.0186)
Constant	0.0306***	0.0289**
	(0.00986)	(0.0113)
Controls	✓	✓
IV	✓	✓
Observations	180,280	181,690
Number of CDP IDs	19,319	19,460

Robust standard errors in parentheses
*** p<0.01, ** p<0.05, * p<0.1

This table presents panel IV regression estimates of individual CDP DAI borrowing, $DAI_{i,t}$, defined as the change in outstanding debt (in millions of DAI). Column (1) uses expected ETH returns from perpetual futures contracts; Column (2) uses a sentiment-based return proxy.
Each specification includes an indicator for extreme negative return episodes—$\mathbf{1}^{(\text{Extreme Neg})}_{\text{perp}} = 1$ if returns fall below -2σ for the perpetual proxy, and $\mathbf{1}^{(\text{Extreme Neg})}_{\text{sent}} = 1$ if returns fall below -1.5σ for the sentiment proxy (a lower threshold is used due to limited extreme observations). We also include an interaction between the ETH return proxy and the respective extreme shock indicator. The regression estimated is:

$$DAI_{i,t} = \alpha_i + \beta_1 \mathbb{E}_t[\tilde{R}^{ETH}] + \beta_2 \mathbf{1}^{(\text{Extreme Neg})} + \beta_3 \mathbb{E}_t[\tilde{R}^{ETH}] \times \mathbf{1}^{(\text{Extreme Neg})} + \beta_4 (p_t^{DAI} - 1) + \text{Controls}_t + u_{i,t}$$

Controls include lagged policy rates, ETH volatility, CDP-specific fees, and instrumented peg deviations. Fixed effects are included at the CDP level. Sample: Nov 18, 2019 – Sep 16, 2024.

C.3 Alternative Collateral Types: WBTC

Figure A3: Distribution of Leverage for WBTC and USDC Vaults

Panel A: WBTC CDPs

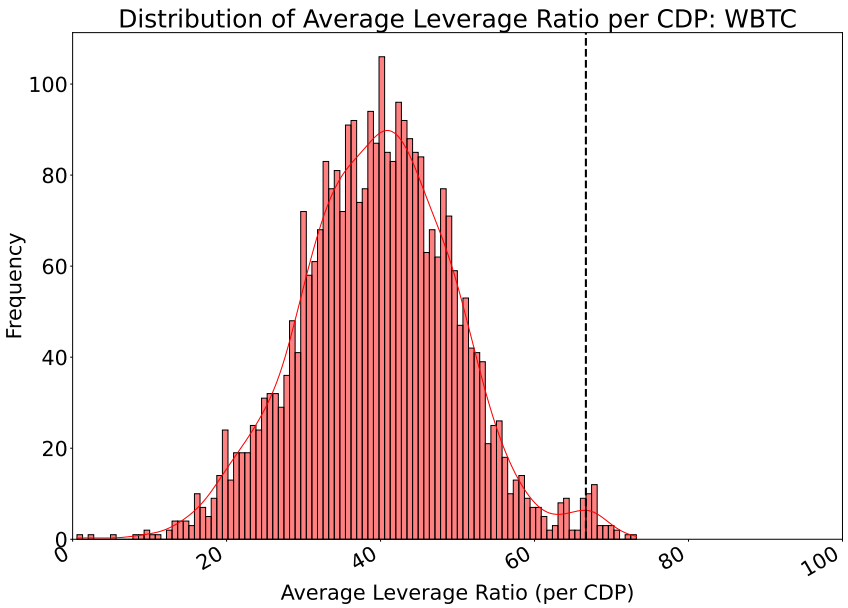

Panel B: CDP #25977: WBTC Speculator

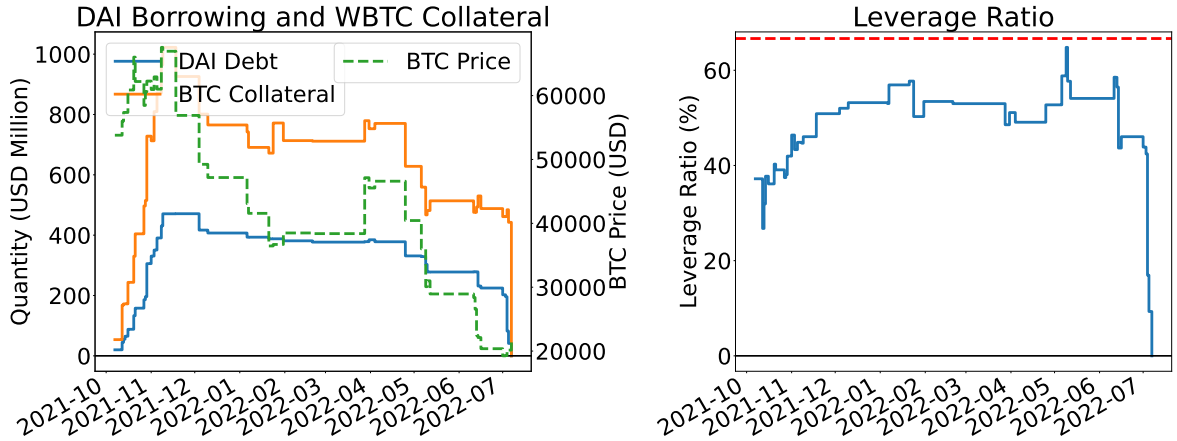

This figure plots measures of leverage across MakerDAO vaults. Panel A shows the distribution of average leverage ratios for all active WBTC CDPs. A CDP is classified as active if it recorded a positive DAI debt balance at any point. The leverage ratio is defined as the ratio of DAI debt to the dollar value of collateral, averaged over the CDP's active period. Panel B plots the time series of DAI borrowings and collateral (left axis) and the leverage ratio (right axis) for CDP #25977, a representative WBTC speculator who borrows DAI to take long leveraged positions in WBTC. The sample period is from 18 November 2019 to 16 September 2024.

Table A3: Determinants of CDP DAI Borrowing - WBTC Collateral

	(1)	(2)	(3)	(4)
	$DAI_{i,t}$			
$\mathbb{E}_t[\tilde{R}^{BTC}_{perp}]$	0.0749***		0.0929**	
	(0.0204)		(0.0455)	
$\mathbb{E}_t[\tilde{R}^{BTC}_{sent}]$		0.204**		0.201**
		(0.0837)		(0.0836)
$\tilde{R}^{BTC}_t$			-0.0234	0.0553***
			(0.0437)	(0.0175)
$p^{DAI}_t - 1$	-0.00394	0.0839*	-0.00312	0.0895*
	(0.0547)	(0.0487)	(0.0548)	(0.0484)
Constant	0.177**	0.112*	0.175**	0.0899
	(0.0892)	(0.0627)	(0.0880)	(0.0623)
Controls	✓	✓	✓	✓
IV	✓	✓	✓	✓
Observations	27,457	27,457	27,457	27,457
Number of CDP IDs	3,114	3,114	3,114	3,114

Robust standard errors in parentheses

*** p<0.01, ** p<0.05, * p<0.1

This table presents panel IV regression estimates of individual CDP DAI borrowing, $DAI_{i,t}$, defined as the change in outstanding debt (in millions of DAI), regressed on BTC return proxies and DAI peg deviations:

$$Y_{i,t} = \alpha_i + \beta_1 \mathbb{E}_t[\tilde{R}^{BTC}] + \beta_2 (p^{DAI}_t - 1) + \text{Controls}_t + u_{i,t},$$

where $\mathbb{E}_t[\tilde{R}^{BTC}]$ represents either expected BTC return from perpetual futures ($\mathbb{E}_t[\tilde{R}^{BTC}_{perp}]$), the sentiment-based proxy $\mathbb{E}_t[\tilde{R}^{BTC}_{sent}]$, or a combination of those with the actual return $\tilde{R}^{BTC}_t$. All return measures are standardized. The variable $p^{DAI}_t - 1$ denotes the deviation of the secondary market DAI/USD price from parity. Control variables include lagged DAI borrowing and savings rates and intraday BTC volatility. Peg-price deviations are instrumented using their lag, BTC returns and volatility, and policy rates. All regressions include CDP fixed effects with standard errors clustered at the CDP level. The sample covers November 18, 2019 to September 16, 2024.

D VAR IRFs

Figure A4: Impulse Responses of DAI Price to ETH Return (Sentiment Proxy), Policy Parameters, Liquidations, Supply and Demand Proxies

Panel A: ETH Return (Sentiment Proxy)

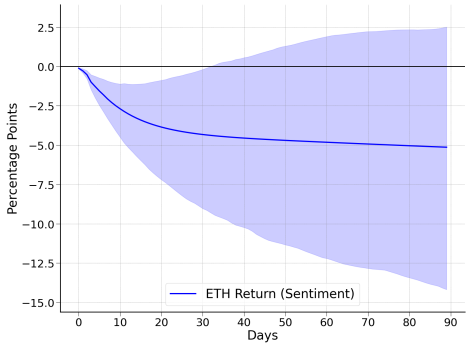

Panel B: Stability Fee (ETH)

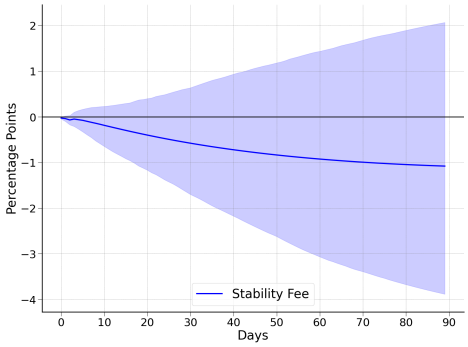

(a) Panel C: DAI Savings Rate (DSR)

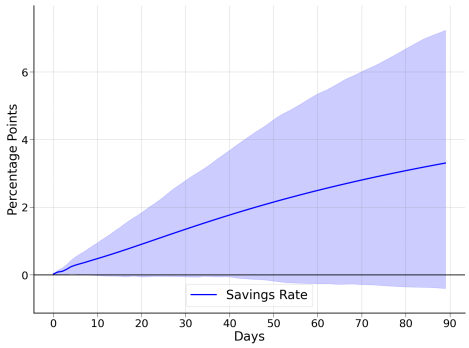

Panel D: Liquidations (ETH)

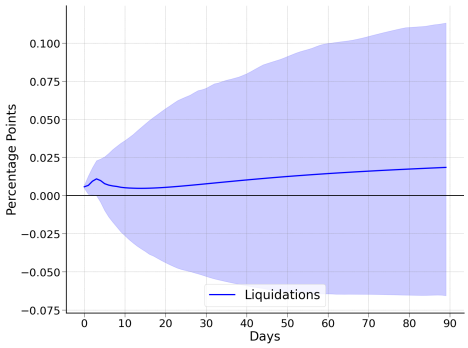

(b) Panel E: DAI Supply

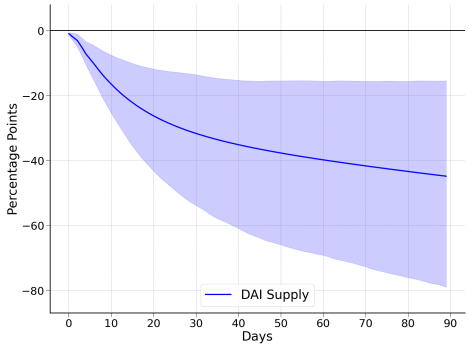

Panel F:DAI Demand Proxy

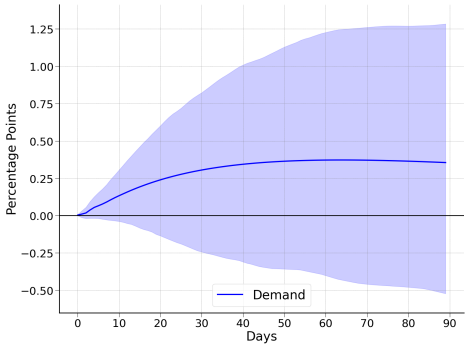

This figure presents the cumulative impulse response functions (IRFs) of the DAI price to shocks in ETH market variables and monetary fundamentals. Panel A shows the effect of expected ETH return shock (sentiment proxy), Panel B the ETH stability fee, and Panel C the DSR. Panels D through F show the effects of ETH-collateral liquidations, log DAI supply, and a DAI demand proxy, respectively. The IRFs are estimated from a structural VAR with 1,000 wild bootstrap replications. Solid lines indicate the mean response, and shaded areas represent 95% confidence bands. The sample spans from 18 November 2019 to 16 September 2024.

E Peg Efficiency: Robustness Tests

E.1 DAI Volatility

Table A4: The Effect of Safe Collateral Composition on DAI Price Volatility

	(1) σ_t^{DAI}	(2) σ_t^{DAI}
Share Safe	-43.719***	
	(5.247)	
Share Safe$_{\text{vault}}$		-30.442***
		(7.026)
Share Safe$_{\text{psm}}$		-43.588***
		(5.235)
σ^{ETH}	0.030***	0.030***
	(0.008)	(0.008)
σ_{t-1}^{DAI}	0.581***	0.579***
	(0.043)	(0.044)
Controls	✓	✓
R^2	0.551	0.551
Observations	1,761	1,761

Robust standard errors in parentheses
*** p<0.01, ** p<0.05, * p<0.1

This table presents OLS regression estimates examining the determinants of DAI price volatility, σ_{DAI}. Column (1) includes the aggregate share of DAI backed by safe collateral. Column (2) separates this into vault-based and PSM-based components. The estimatxed model is:

$$\sigma_{\text{DAI},t} = \alpha + \beta_1 \text{ShareSafe}_t^{(i)} + \text{Controls}_t + \varepsilon_t,$$

where $\text{ShareSafe}_t^{(i)}$ denotes the time-t share of stablecoin-backed DAI. ETH volatility (σ_{ETH}) and lagged DAI volatility are shown; other controls (included but omitted from the table) are the DAI Stability Fee, ETH Liquidations, Stability Fees on ETH CDPs, and DAI Velocity. Standard errors are robust to heteroscedasticity. The sample spans November 18, 2019 to September 16, 2024.

E.2 Estimating Arbitrage Bounds

In Figure 1, we show that peg premiums became significantly more compressed following the introduction of the PSM. Summary statistics in Table 3 indicate that average peg deviations were substantially higher prior to the PSM, and declined markedly thereafter. As shown in our empirical analysis in Section 5.2.4, access to the PSM compresses peg premiums by providing arbitrageurs with an effective mechanism to supply DAI when it

trades at a premium—specifically, by allowing them to swap USDC for DAI at a 1:1 rate and sell the DAI in the secondary market.

To formally test for asymmetries in peg-price deviations across regimes, and to evaluate the stabilizing role of the PSM, we estimate a Self-Exciting Threshold AutoRegressive (SETAR) model. SETAR models are commonly used to identify regime-dependent dynamics in time series and have been applied in macro-finance to study shifts in exchange rate dynamics, capital control regimes, and speculative pressure episodes (Clements and Smith, 2001; Chappell et al., 1996; Hutchison, Pasricha, and Singh, 2012).

In our context, we hypothesize that the dynamics of peg-price deviations $\Delta_{DAI,t}$ are regime-dependent, with arbitrageurs better able to correct DAI premiums following the launch of the PSM. We estimate Equation (57) separately for the pre- and post-PSM periods. The model allows for three autoregressive processes depending on the magnitude of the lagged peg deviation, with the middle regime interpreted as a "band of inaction" where arbitrage incentives are weak or absent.[24]

$$\Delta_{DAI,t} = \begin{cases} \rho_L \Delta_{DAI,t-1} + \epsilon_t, & \Delta_{DAI,t-1} < \Delta_L \\ \rho_M \Delta_{DAI,t-1} + \epsilon_t, & \Delta_L \leq \Delta_{DAI,t-1} \leq \Delta_U \\ \rho_U \Delta_{DAI,t-1} + \epsilon_t, & \Delta_{DAI,t-1} > \Delta_U \end{cases} \tag{57}$$

Results are presented in Table A5. In the pre-PSM period, the band of inaction spans from -8 to 287 basis points, indicating that arbitrageurs required relatively large peg premiums to be incentivized to supply DAI. Above 287 bps, the estimated autoregressive coefficient $\rho_U = 0.687$ implies a half-life of roughly 2.51 days, consistent with slow mean reversion.

In contrast, the post-PSM regime shows a much tighter band of inaction—from 1 to 27 basis points—reflecting improved arbitrage efficiency due to the introduction of the PSM. The estimate $\rho_U = 0.402$ implies a much faster half-life of 0.78 days, indicating that large peg deviations are now corrected more rapidly. In particular, our findings suggest that the PSM compresses peg premiums and improves peg stability by enabling a more effective arbitrage response.

24. The low regime is defined as $\Delta_{DAI,t-1} < \Delta_L$, the middle regime as $\Delta_L \leq \Delta_{DAI,t-1} \leq \Delta_U$, and the high regime as $\Delta_{DAI,t-1} > \Delta_U$. See Hansen (1999) for further details.

Table A5: SETAR of Peg Deviations Pre- and Post-PSM Periods

Period	ρ_L	ρ_M	ρ_U	Δ_L	Δ_U
Pre-PSM	-0.074	1.021	0.687	-8bps	287bps
Post-PSM	-0.228	0.946	0.402	1bps	27bps

This table presents results from estimating a Self-Exciting Threshold AutoRegressive (SETAR) model for DAI peg-price deviations. Each row reports autoregressive coefficients ρ and threshold values for the low (Δ_L) and high (Δ_U) regimes. The sample for the pre-PSM period runs from 18 November 2019 to 17 December 2020, while the post-PSM period runs from 18 December 2020 to 16 September 2024.